BMC Materials

REVIEW

Open Access

Noble metal-free two dimensional carbon-based electrocatalysts for water splitting

Muhammad Adnan Younis[1†], Siliu Lyu[1†], Qidong Zhao[4], Chaojun Lei[1], Peiling Zhang[4], Bin Yang[1], Zhongjian Li[1], Lecheng Lei[1], Yang Hou[1,3,5*] and Xinliang Feng[2]

Abstract

Noble metal materials are widely employed as benchmark electrocatalysts to achieve electrochemical water splitting which comprises of hydrogen evolution reaction (HER) and oxygen evolution reaction (OER). However, the high cost and scarcity limit the wide ranging commercial applications of noble metal-based catalysts. Development of noble metal-free two dimensional (2D) carbon-based materials can not only reduce the consumption of noble metals, but also create materials with the characteristics of high active surface area, abundance, easy functionalization, and chemical stability, which may carve a way to promising electrochemical water splitting. In this review, noble metal-free 2D carbon-based electrocatalysts, including heteroatom (B, S, N, P, F, and O) doped graphene, 2D porous carbons modified with heteroatoms and/or transition metals, and 2D carbon-based hybrids are introduced as cost-effective alternatives to the noble metal-based electrocatalysts with comparable efficiencies to conduct HER, OER, and overall water splitting. This review emphasizes on current development in synthetic strategies and structure–property relationships of noble metal-free 2D carbon-based electrocatalysts, together with major challenges and perspectives of noble metal-free 2D carbon-based electrocatalysts for further electrochemical applications.

Keywords: 2D nanocarbons, Noble metal-free electrocatalysts, Hydrogen evolution reaction, Oxygen evolution reaction, Overall water splitting

Introduction

Electrochemical water splitting is found to be an exciting approach for energy conversion due to its negligible environment pollution and high energy conversion efficiency. Generally, electrochemical water splitting process comprises of two half reactions, which include hydrogen evolution reaction (HER) at cathode and oxygen evolution reaction (OER) at anode, respectively. An ideal HER or OER catalyst must be active for each half reaction with excellent stability. Currently, the materials containing expensive noble metals (Pt, Ir, or Ru) are emerged as the most commonly used electrocatalysts for water splitting, but their high price and scarcity seriously restrict their widespread applications [1–7]. Therefore, the development of alternative noble metal-free electrocatalysts with acceptable electrochemical performances, low cost, and long-term durability is highly desirable but remains challenging [8–10]. In order to overcome such challenges, many efforts have been exercised to design noble metal-free electrocatalysts, including transition metal carbides, nitrides, phosphides, and chalcogenides to conduct HER, and transition metal phosphates, oxides, perovskites, hydroxides, nitrides, and chalcogenides for OER, but the low conductivity, aggregation, and less stability in acidic and basic solutions limit their large scale applications [11–24].

Recently, noble metal-free nanocarbon-based materials, such as zero dimensional (0D) fullerenes, one dimensional (1D) carbon nanorods, 1D carbon nanotubes (CNTs), two dimensional (2D) modified graphene, 2D porous carbon nanosheets (PCNs), and carbon frameworks with three dimensional (3D) structures, etc., have been employed as cost-effective alternatives to traditional noble-metal catalysts for electrochemical water splitting [25–34]. Among them, 2D nanocarbons possess unique

*Correspondence: yhou@zju.edu.cn
†Muhammad Adnan Younis and Siliu Lyu contributed equally
[5] Ningbo Research Institute, Zhejiang University, Ningbo 315100, China
Full list of author information is available at the end of the article

layered structure, unusual physical, chemical and electronic characteristics, as well as highly exposed active site, which make them attractive candidates for electrocatalytic applications [31]. For example, 2D graphene offers a remarkable mechanical strength, exceptionally higher carrier mobility of ~ 15,000 cm^2 V^{-1} s^{-1} at room temperature, and better optical transparency of ~ 97.7% than 0D fullerene [35]. In addition, 2D graphene has extremely good electrical conductivity of 64 mS cm^{-1} and excellent thermal conductivity of 5000 W m^{-1} K^{-1} as compared to 1D single walled CNTs (~ 1.06 mS cm^{-1} and ~ 3000 W m^{-1} K^{-1}, respectively) [27, 35–42]. While, 2D porous carbons may have more accessible active sites due to unique layered structure and effectively prevent irreversible restacking and overlapping as compared to 3D nanostructured materials [31, 43]. Overall, the 2D nanocarbons possess highly opened-up flat structures and large surface areas, which may provide the rapid contact of the catalyst with the reactants, short ion/mass transport distances and continuous electron transport pathways, thus leading to high electrocatalytic activities [43]. Such characteristics enable 2D structured nanocarbons to be used as economical and competent metal-free electrocatalysts or good supports for transition metal compounds and metal-free materials in energy conversion systems. As far as we know, the exploration of nanocarbon-based electrocatalysts has attained wide attention, and few review articles have already discussed the modified carbons and carbon-based hybrids for electrochemical water splitting [44–51]. However, comprehensive reviews that summarize recent developments of noble metal-free 2D carbon-based electrocatalysts including the synthetic methods and structure–activity relationships still remain missing.

In this review, the development of recent reported noble metal-free 2D carbon-based electrocatalysts, including heteroatom-doped graphene, 2D porous carbons modified with heteroatoms and/or transition metals, and 2D carbon-based hybrids towards HER, OER, and overall water splitting are summarized (Fig. 1). A concise summary on the synthetic methods and electrocatalytic performances of noble metal-free 2D carbon-based electrocatalysts for HER, OER, and overall water splitting are given in Tables 1, 2, and 3, respectively. In final section, the major challenges and perspectives for further research on noble metal-free 2D carbon-based electrocatalysts are discussed.

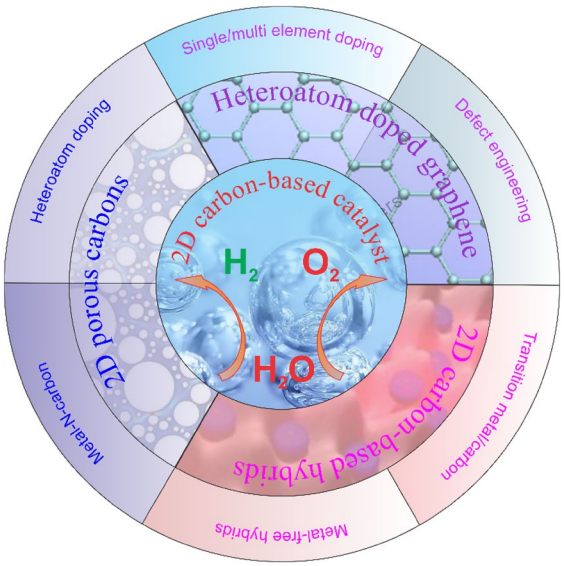

Fig. 1 Schematic representation of the noble metal-free 2D carbon-based electrocatalysts for water splitting, classified according to the type of electrocatalysts discussed in this manuscript. The center shows the demonstration of water splitting by noble metal-free 2D carbon-based electrocatalysts

2D carbon-based electrocatalysts for water splitting

Since 2004, the successful preparation of graphene having one-atom-thickness and crystalline sp2-carbon sheet opens a new era of exploration of 2D carbon-based materials [37, 52]. The 2D carbon-based materials, such as heteroatom-doped graphene, 2D porous carbons modified with heteroatoms and/or transition metals, and 2D carbon-based hybrids have instigated immense interest because of their dangling groups, intrinsic, structural, and unique surface properties, which may provide high adsorption/desorption ability toward the key reaction intermediates during water electrocatalysis [53].

Among these 2D nanocarbons, heteroatom (B, S, N, P, F, and O) doped graphene-based electrocatalysts possess remarkable physical and chemical characteristics with modified electronic structures and abundant exposed active sites, which might be beneficial to catalyze HER, OER, and overall water splitting [33, 44, 54–56]. While, 2D porous carbon-based catalysts including heteroatoms and/or transition metals doped porous carbons exhibit large surface area and high porosity, leading to the rapid diffusion of chemical species to and from the surface of electrocatalysts during electrochemical reactions, which is important for superior catalytic performances [31, 57–59]. Additionally, the 2D carbon-based hybrids (2D nanocarbons with transition metal compounds and metal-free materials) possess excellent water splitting activities owing to the remarkable advantages of promising catalytic abilities of transition metal compounds and other metal-free substances as well as high conductive carbon supports, which may enhance the capabilities of such hybrids for electrochemical applications [60, 61]. Conclusively, the

Table 1 Summary of noble metal-free 2D carbon-based electrocatalysts for HER

Material	Application	Synthesis method	Electrolyte	Onset potential versus RHE (V)	Over potential versus RHE (V)	Tafel slope (mV dec^{-1})	References
B-doped graphene	HER	Sonication	0.5 M H_2SO_4	0.30	0.47	130	[66]
S-doped graphene	HER	Pyrolysis	0.5 M H_2SO_4	–	0.57	78	[71]
NMPG	HER	Pyrolysis	0.5 M H_2SO_4	–	0.23	109	[170]
N,P/graphene	HER	Annealing	0.5 M H_2SO_4	–	0.42	91	[75]
N,P/graphene	HER	Pyrolysis	0.5 M H_2SO_4	–	0.37	89	[171]
N,S/graphene	HER	CVD	0.5 M H_2SO_4	0.13	0.28	80.5	[172]
N,S/graphene	HER	Sonication	0.5 M H_2SO_4	–	0.30	120	[74]
N,B-graphene	HER	Annealing	0.1 M KOH	–	0.17	82.1	[86]
CoNi/NC	HER	Annealing	0.1 M H_2SO_4	–	0.14	105	[173]
CoP/carbon	HER	Hydrothermal	0.5 M H_2SO_4	0.07	0.11	56.7	[174]
Co/N-doped carbon	HER	Hydrothermal	0.1 M KOH	0.06	0.25	126	[175]
VCN/Fe_4N	HER	Carbonization	0.1 M KOH	–	0.17	80	[153]
Defect graphene	HER	Annealing	0.5 M H_2SO_4	–	1.5	55	[85]
Ni@NC	HER	Annealing	1.0 M KOH	0.07	0.2	160	[176]
Fe_3C-graphene	HER	CVD	0.5 M H_2SO_4	–	49	46	[177]
Mo_2C/NC	HER	Pyrolysis	1.0 M KOH	–	60	60	[178]
N,S/carbon	HER	Pyrolysis	0.5 M H_2SO_4	–	0.1	57.4	[107]

Table 2 Summary of noble metal-free 2D carbon-based electrocatalysts for OER

Material	Application	Synthesis method	Electrolyte	Onset potential versus RHE (V)	Over potential versus RHE (V)	Tafel slope (mV dec^{-1})	References
NPF-Graphene	OER	Annealing	0.1 M KOH	1.62	1.82	136	[89]
N-GRW	OER	Pyrolysis	1.0 M KOH	–	0.36	47	[81]
NFGN	OER	Annealing	1.0 M KOH	1.45	1.55	78	[90]
NMG	OER	CVD	0.1 M KOH	–	1.66	–	[82]
EG/$Co(OH)_2$	OER	Hydrothermal	1.0 M KOH	–	1.53	63	[135]
BN-NC	OER	Annealing	0.1 M KOH	–	1.65	–	[86]
CQD/Graphene	OER	Solvothermal	1.0 M KOH	–	1.57	44	[179]
N-carbon	OER	Pyrolysis	1.0 M KOH	–	0.38	–	[109]
FeN_4/CF/EG	OER	Carbonization	0.5 M H_2SO_4	–	0.29	129	[6]
Co-BNC	OER	Carbonization	1.0 M KOH	–	0.30	70	[180]
Co-Graphene	OER	Soft template	0.1 M KOH	–	0.35	83.3	[115]
Co_3O_4/GCN	OER	Annealing	0.1 M KOH	–	0.12	76	[181]
N-doped graphene	OER	CVD	0.1 M KOH	–	1.6	83	[30]
CoP/N,P-Graphene	OER	Pyrolysis	1.0 M KOH	–	0.27	54	[149]
N,P-graphene	OER	Pyrolysis	0.1 M KOH	–	1.57	70	[87]
VCN/FeOOH	OER	Carbonization	0.1 M KOH	–	0.17	57	[153]
Defect graphene	OER	Annealing	1.0 M KOH	–	1.57	97	[85]
Ni@NC	OER	Annealing	1.0 M KOH	–	0.28	45	[176]
Co_3O_4/NPC	OER	Carbonization	0.1 M KOH	1.47	1.5	70	[182]

outstanding physical and chemical properties of above-mentioned 2D nanocarbon-based materials make them potential candidates to conduct electrochemical water splitting, which involves HER at cathode and OER at anode. The overall reaction during electrochemical water splitting in an electrolytic cell is as follows:

Total reaction

Table 3 Summary of noble metal-free 2D carbon-based electrocatalysts for overall water splitting

Material	Synthetic method	Electrolyte	Overall potential versus RHE (V)	References
NFGNs	Chemical method	1.0 M KOH	1.90	[90]
Ni@NC	Annealing	1.0 M KOH	1.60	[66]
NiFe/NC	Pyrolysis	1.0 M KOH	1.58	[183]
N-graphene/CoO	Solvothermal	1.0 M KOH	1.58	[184]
DRPC	Template	1.0 M KOH	1.53	[117]
N-carbon	CPT	0.1 M KOH	1.82	[118]
CoO/NC	Pyrolysis	1.0 M KOH	1.55	[151]
CoP/NC	Annealing	1.0 M KOH	1.73	[147]
CoP/rGO	Annealing/phosphoration	1.0 M KOH	1.56	[138]
CoP/rGO	Pyrolysis	1.0 M KOH	0.47	[145]
Co-BNC	Carbonization	1.0 M KOH	1.68	[180]
CoP/NPMG	Carbonization	1.0 M KOH	1.60	[149]
NiP/C	Electrodeposition/phosphoration	1.0 M KOH	1.63	[146]
VCN@Fe_4N/FeOOH	Annealing	0.1 M KOH	1.60	[153]
NiFe-LDH NS@DG	Suspension	1.0 M KOH	1.50	[156]

$$H_2O \rightarrow H_2 + 1/2\,O_2 \quad (1)$$

Hydrogen (H_2) production by using electrochemical methods was regarded as the most exciting alternative solution to solve the present energy related issues by virtue of negligible pollution, high energy conversion efficiency, and minimum cost [62]. At cathode, the H_2 evolves during water splitting, and the HER mechanism is mainly based on two steps, the first of which is Volmer reaction and the second is Heyrovsky reaction/Tafel reaction [10]. In the first step, the Volmer reaction consists of the adsorption of both H^+ and an e^- on the surface of electrocatalysts in acidic, neutral, or basic solutions. The second step may belong to two different pathways. One is the adsorption of H^+ with e^- and the other belongs to the addition of two adsorbed H to produce one molecule of H_2. The kinetics of the HER can be affected by the nature of the catalyst. The overall reactions for H_2 production in different solutions are as follows:

In acidic electrolytes:

$$\text{Cathode } 2H^+ + 2e^- \rightarrow H_2 \quad (2)$$

In basic or neutral electrolytes:

$$\text{Cathode } 2H_2O + 2e^- \rightarrow H_2 + 2OH^- \quad (3)$$

While at anode, the oxygen (O_2) evolves during water splitting, and the OER mechanism involves four electron transfer process and generates multiple reaction intermediates, such as OH*, O*, and OOH* in acidic, neutral or basic solutions [10]. The overall reactions associated with O_2 production in different media are given as below:

In acidic electrolytes:

$$\text{Anode } H_2O \rightarrow 2H^+ + 1/2O_2 + 2e^- \quad (4)$$

In basic or neutral electrolytes:

$$\text{Anode } 2OH^- \rightarrow H_2O + 1/2O_2 + 2e^- \quad (5)$$

Both HER and OER during electrochemical water splitting require considerable overpotential and suffer from sluggish kinetics, and thus, the advancement of noble metal-free 2D carbon-based electrocatalysts to conduct HER, OER, and overall water splitting with maximum efficiency has gained enormous attention.

Heteroatom-doped graphene-based electrocatalysts for water splitting

Among 2D nanocarbons, heteroatom-doped graphene based electrocatalysts have attained great attention for multiple electrochemical applications due to their promising electronic and mechanical properties, including high conductivity and tensile strength. As is known, the electrochemical inertness of graphene limits its practical applications to conduct electrochemical water splitting. However, the heteroatom (B, S, N, P, F, and O) doping of graphene, reduced graphene oxide (rGO), graphene oxide (GO), and electrochemical exfoliation of graphite provide ample opportunities to develop heteroatom-doped graphene based electrocatalysts [63, 64]. The heteroatoms of B, S, N, P, F, and O hold great potential to alter the intrinsic properties of graphene based materials and enable them to adsorb reactant species on their surface without disturbing their electrical conductivities, which shows the availability of foundation for unusual catalytic performances [65–68]. Furthermore, it has

been noted that the modification of graphene via high electronegative heteroatom (e.g., N, F, and O) doping can easily modulate the electronic structures by activating the adjacent carbon atoms in the graphene, leading to increase catalytic sites, which ultimately boosts up the electrochemical activities for water splitting [69]. In addition, the co-doping with higher and lower electronegative heteroatoms can also provide a synergistic effect between heteroatoms with a distinctive electronic structure and consequently enhance the activity of heteroatom-doped graphene-based electrocatalysts [70].

Heteroatom-doped graphene-based electrocatalysts for hydrogen evolution reaction

Owing to the remarkable properties, including good thermal stability, high electrical conductivity, and easily tunable electronic structure, the electrocatalysts based on heteroatom (B, S, N, and P) doped graphene, have shown promising potential for electrocatalytic HER. For instance, a B-doped graphene developed from defective graphene was synthesized by using wet chemical synthetic approach (Fig. 2a) [66]. The as-prepared B-doped graphene acted as HER electrocatalyst in acidic electrolyte possessed a Tafel slope of 130 mV dec^{-1}. Additionally, the further electrochemical measurements proposed that the B-doped graphene required a smaller overpotential of ~ 0.45 V at 10 mA cm^{-2}, as compared to the defective graphene (~ 0.51 V). The synergistic effect of B atoms and graphene were found responsible in the enhancement of HER activity of B-doped graphene. In another study, a S-doped graphene was developed by annealing treatment of GO with Na_2S at 1000 °C, and their HER catalytic activities were observed in 0.5 M H_2SO_4 [71]. The S-doped graphene designed at 1000 °C showed a Tafel slope of 128 mV dec^{-1}, whilst the S-doped graphene electrocatalyst displayed a low overpotential of ~ 0.57 V to reach up to 10 mA cm^{-2}, demonstrating reasonable catalytic property towards HER. Moreover, the HER performance of S-doped graphene prepared at 1000 °C was compared with that of graphene sheets, which obtained the 10 mA cm^{-2} with slightly higher overpotential of ~ 0.64 V. Decisively, the high HER activity of S-doped graphene was endorsed by the synergistic effect of S-dopant and graphene nanosheets.

Among various heteroatom (B, S, and N) dopants, the doping with N atom provides stronger affinity for H atom, as N-dopant can alter the energy levels of graphene matrix by activating the adjacent carbon atoms, leading to boosted interaction between the N-doped graphene and catalytic intermediate (H*), which ultimately reduces the H* species to H_2. Hence, construction of heteroatom-doped graphene with N-doping provides an impressive direction to upheld the catalytic activity of electrocatalyst for HER [72]. In this regard, a N-doped mesoporous graphene (NMPG) was developed via a simple pyrolysis treatment of GO and cyanimide at 800 °C for HER [72]. The as-prepared NMPG possessed outstanding high surface area of ~ 927 m^2 g^{-1} along with high porosity of ~ 3.3 cm^3 g^{-1}. Acting as a HER electrocatalyst, the NMPG demonstrated a Tafel slope of 109 mV dec^{-1}. Moreover, the further electrochemical results showed that the NMPG displayed the current density of 10 mA cm^{-2} with a low overpotential of ~ 0.24 V, when using acidic medium as an electrolyte. In contrast, the negligible HER catalytic properties of dopant-free mesoporous graphene and pristine graphene were observed in same acidic electrolyte. More evidences described that the synergistic effect of N-doping and mesoporous structure remarkably improved the HER activity of NMPG.

Besides the single-atom doped graphene, the further researches indicated that the improvement in HER performance can be made by the introduction of more than one heteroatom, such as N/P or N/S, as multi-atom doping gives rise to the synergistic effect, leading to the improved HER [73, 74]. Thus, to further enhance the catalytic activity, the heteroatom co-doping approach was utilized to prepare an efficient N, P co-doped graphene, which was fabricated via a carbonization treatment of GO by using N and P precursors at 950 °C for HER [75]. The N, P co-doped graphene represented Tafel slopes of 91 and 145 mV dec^{-1} along with the overpotentials of 0.42 V and 0.585 V at 10 mA cm^{-2}, when adopting the acidic and basic electrolyte, respectively. Furthermore, the overpotential of N, P co-doped graphene was relatively smaller than that of N-doped graphene (~ 0.49 V) and P-doped graphene (~ 0.55 V) in acidic media. Convincingly, the N, P co-dopants might activate the neighboring carbon atoms and thus generate additional active sites, which raised the HER property of heteroatom-doped graphene. Besides the N, P heteroatoms, the co-doping of graphene with N, S dopants, was also found to be an alternatively effective strategy. In this regard, an electrocatalyst consisting of graphene with multi-atom combination of N, S dopants by annealing treatment of GO, benzyl disulfide, and melamine at 900 °C was developed to conduct HER, as shown in Fig. 2b [74]. The N, S-doped graphene showed Tafel slope of 120 mV dec^{-1} during HER. Moreover, the N, S-doped graphene displayed the current density of 10 mA cm^{-2} by yielding significantly small overpotential of ~ 0.31 V in 0.5 M H_2SO_4, which was noticeably smaller than that of the N-doped graphene (~ 0.49 V), N, P-doped graphene (~ 0.49 V), and N, B-doped graphene (~ 0.54 V) (Fig. 2c). Convincingly, the interplay of negatively charged S dopants and positively charged N dopants provided geometric lattice

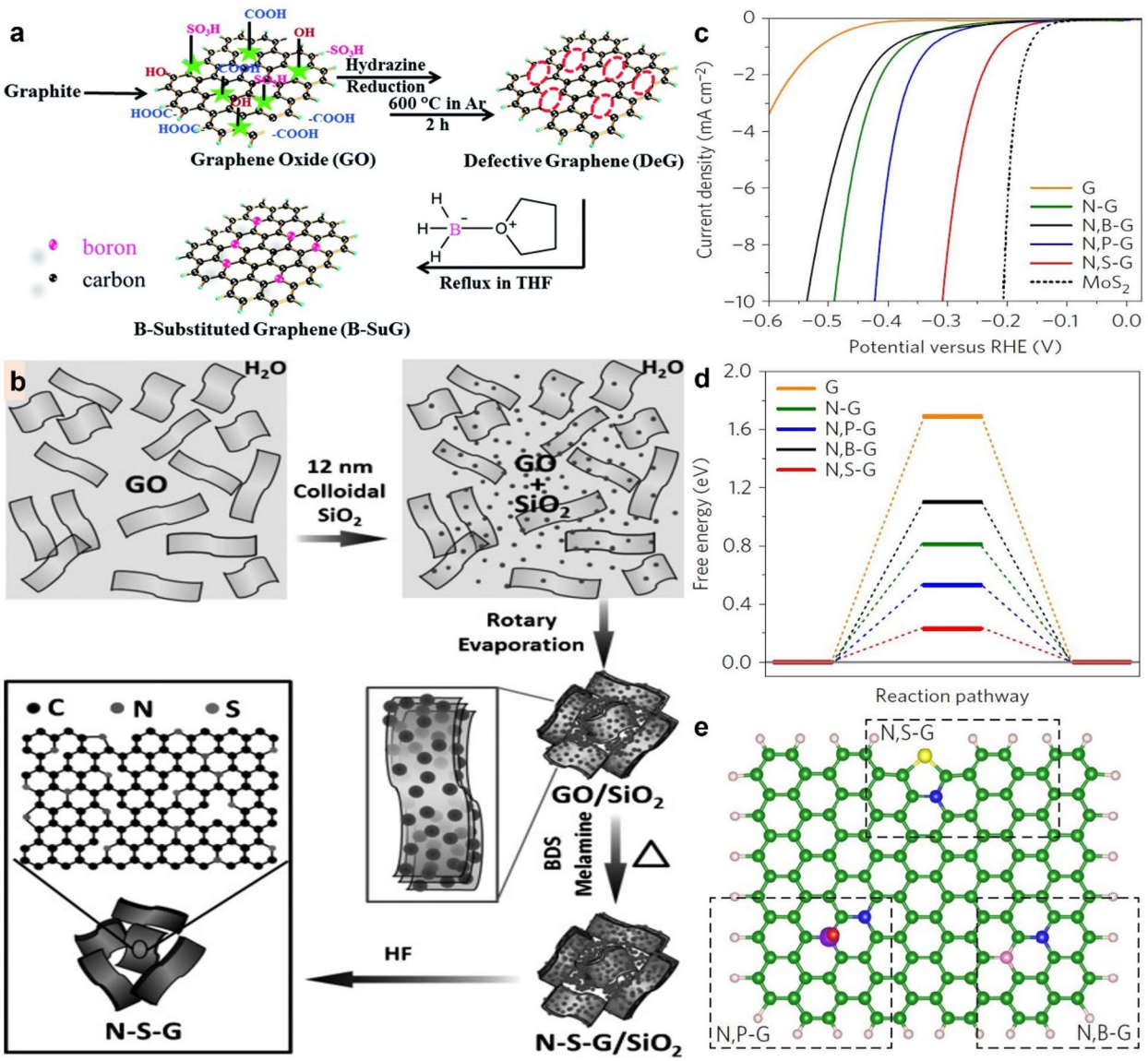

Fig. 2 **a** Schematic representation of the synthetic process of B-substituted graphene. Reproduced with permission from Ref. [66]. Copyright 2017, Royal Society of Chemistry. **b** Illustration of the synthetic route to design N, S doped graphene. Reproduced with permission from Ref. [73]. Copyright 2012, Wiley-VCH. **c** Comparison of MoS_2 with different graphene-based electrocatalysts in 0.5 M H_2SO_4. **d** Free energy diagram of pure, single and co-doped graphene. **e** Atomic representation of co-doped models and their corresponding ΔG_{H^*}. **c**–**e** Reproduced with permission from Ref. [74]. Copyright 2016, Nature Publishing Group

defects and rapid electron transfer paths, which play vital role in improving the activity of N, S-doped graphene for HER (Fig. 2d, e).

From the above, it is clear that the heteroatom doping with single heteroatoms or multi-atoms performed a meaningful role in tuning the electronic structure of 2D graphene-based electrocatalysts, resulting in strong adsorption for H*, which lead to the remarkable HER performances. Additionally, the multi-atoms doped graphene based electrocatalysts were found to have higher catalytic abilities and more active sites as compared to single heteroatom-doped graphene-based electrocatalysts. Thus, development of heteroatom co-doped graphene electrocatalysts may be an exciting direction for further research in the sustainable H_2 production [74, 76–80].

Heteroatom-doped graphene-based electrocatalysts for oxygen evolution reaction

The efficiencies of electrochemical water splitting devices can be strongly affected by anode reaction because of the

high overpotentials and sluggish kinetics of OER process. Nowadays, the noble metal-based oxides (IrO_2 and RuO_2) are still the most competent electrocatalysts for OER, but the expenditure and low natural abundance limit their wide range industrialization. Therefore, researchers have made significant efforts to design heteroatom-doped graphene based electrocatalysts for OER to take over noble metal-based electrocatalysts.

Recent heteroatom-doped graphene, especially N-doped graphene have attained wide spread attention, as the incorporation of N-dopant may modify the chemical reactivity and electronic property of graphene, leading to adsorption of intermediate species (O*), which ultimately enhanced the catalytic ability of N-doped graphene for OER (Fig. 3a). To be specific, the N-doping into graphene matrix can provide the contents of pyrrolic N, quaternary N, and pyridinic N along with oxidized N. Among these N-functionalities, pyridinic N has a lone pair of electrons, which can contribute to resonance in the delocalization of electrons and become electron deficient. Due to this deficiency, pyridinic N atoms accept electrons from neighboring carbon atoms and enable them to adsorb OH^- and OOH^- intermediate species, which was recognized as the rate-determining step during OER. Thus, it is highly anticipated to synthesize electrocatalysts enriched with pyridinic N to achieve desirable OER performances [81–83]. For instance, pyridinic-N dominated doped graphenes (NDGs) with vacancy defects were prepared by hydrothermal method of g-C_3N_4 and GO, followed by pyrolysis treatment from 600 to 900 °C for OER [84]. The NDG prepared at 800 °C exhibited remarkable OER performance by achieving a Tafel slope of 132 mV dec^{-1}. In contrast, the other electrocatalysts prepared at the temperatures of 900 °C and 700 °C demonstrated the higher Tafel slopes, which were 149 and 157 mV dec^{-1}, respectively. Additionally, the NDG prepared at 800 °C showed the potential of ~ 1.67 V with 10 mA cm^{-2}, suggesting an appreciable OER activity. Consequently, the pyridinic N doped carbon sites and vacancy defects synergistically boosted the OER performance of the NDG prepared at 800 °C.

Accordingly, a 2D graphene with carbon defects was developed by using thermal treatment of N-doped graphene at 1150 °C (Fig. 3b) [85]. The defective graphene showed good OER performances with a Tafel slope of 97 mV dec^{-1}. Meanwhile, the defective graphene required a potential of 1.57 V to reach the current density of 10 mA cm^{-2}, which was analogous to commercial Ir/C (~ 1.55 V) in basic media. Eventually, the high OER performances of defective graphene were accredited to the edge defects, which emerged after the subtraction of N atom. The N atom was subtracted from carbon lattice under high energy to create vacant sites and allowed to form low energy defective structures, such as pentagons and octagons, etc. Furthermore, several computational models were studied to describe the types of defects in N-doped graphene. The calculations of energy pathways for five different defective atomic active sites edges were investigated, several of which were attributed to demonstrate high OER performances.

Apart from single atom doping, multiple combinations of dopants (N/P and N/S) with different electronegativity could provide more active centers than single heteroatom dopant, which may raise the electrocatalytic performance for OER [86]. For example, a N, P-doped graphene with surface area of 900.2 m^2 g^{-1} was investigated by pyrolysis treatment of GO sheets and polyaniline (PANI) at 850 °C (Fig. 3c) [87]. The N, P co-doped graphene showed a small Tafel slope of 70 mV dec^{-1} in alkaline solution. Also, the further results indicated that the N, P co-doped graphene required a small potential 1.57 V to reach up to 10 mA cm^{-2} (Fig. 3d, e). Moreover, the N, P co-doped graphene (1.57 V) indicated the superior OER catalytic activities than RuO_2 and Pt/C, the potentials of which were 1.59 V and ~ 2 V, respectively. Accordingly, the synergistic effect, large surface area, and abundantly exposed active sites, were associated to the satisfactory catalytic activity, which provided easy access to reactant molecules and accommodated rapid charge transfer to conduct OER. Subsequently, as promising OER electrocatalyst, a N, S-doped graphene with porous structure and surface area of 554.4 m^2 g^{-1} was developed by a one-pot calcination treatment of GO at 800 °C, followed by a surface activation process with $ZnCl_2$ [88]. When the N, S co-doped graphene with high porosity were used to conduct OER in 1.0 M KOH, it demonstrated a low Tafel slope of 114 mV dec^{-1}. Along with this, the N, S-doped graphene also showed a significantly low potential of ~ 1.55 V at 10 mA cm^{-2}, which further confirmed its better OER activity than other controlled samples. For instance, the N, S-doped graphene without surface activation presented a high Tafel slope of 168 mV dec^{-1} accompanied with large potential of ~ 1.7 V to gain 10 mA cm^{-2}. Eventually, the activation process provided the defects and created numerous active sites, which exceptionally boosted the OER activity of N, S-doped graphene.

Additionally, a tri-doped graphene with N, P, and F atoms was synthesized by using pyrolysis of PANI coated on GO and ammonium hexafluorophosphate at 950 °C [89]. The tri-doped graphene demonstrated the lower Tafel slope of 136 mV dec^{-1} than the RuO_2 (141 mV dec^{-1}) to conduct OER. Furthermore, the onset potential displayed by the tri-doped graphene was approximately 1.62 V in 0.1 M KOH, which was slightly higher than that of RuO_2 (1.53 V). It was suggested that the tri-doped graphene possessed

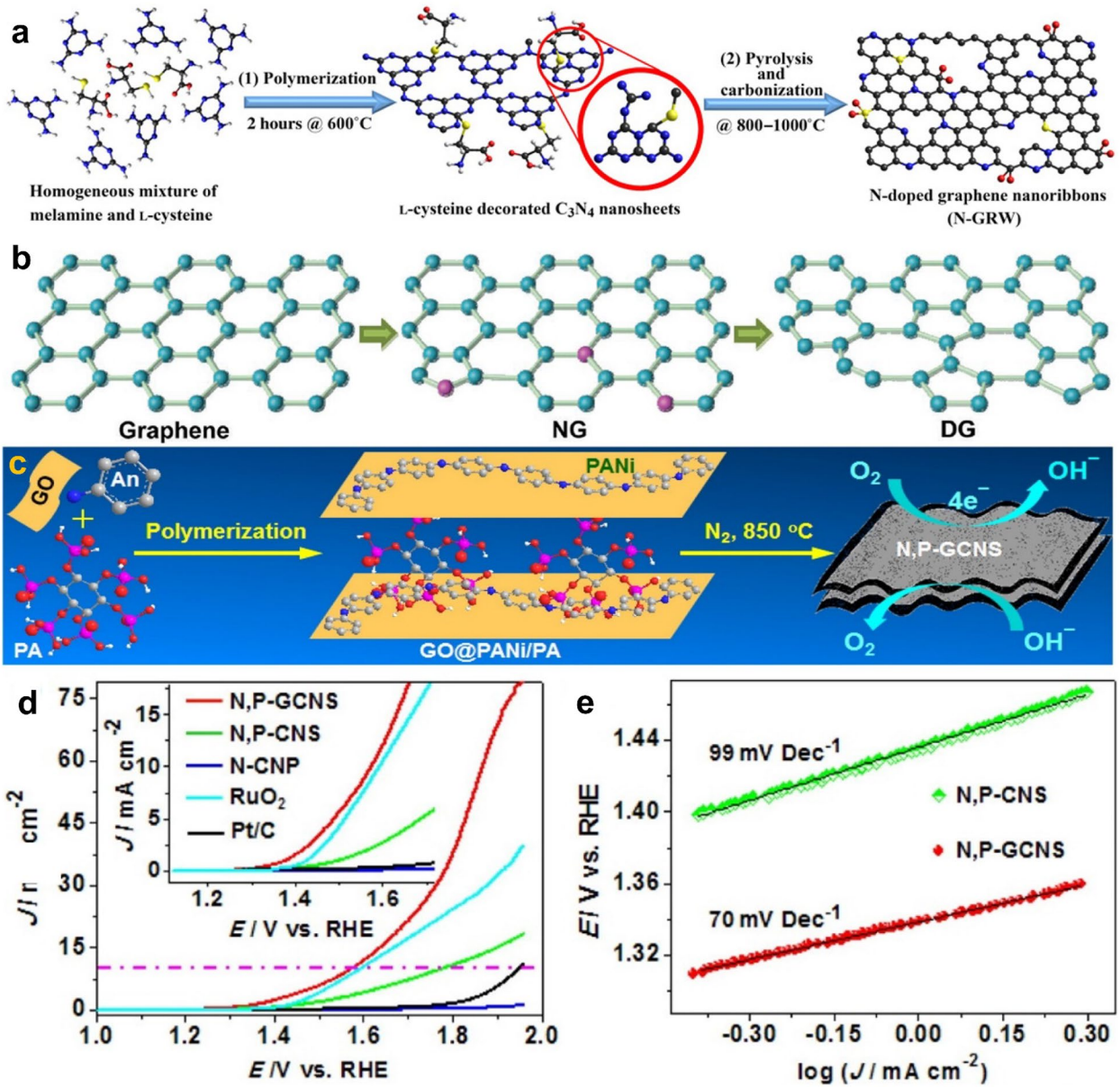

Fig. 3 **a** Synthesis of N-doped graphene by using polymerization method followed by carbonization from 800 to 1000 °C. Reproduced with permissions from Ref. [81]. Copyright 2016, AAAS Science. **b** Illustration of the synthetic process of defective graphene. Reproduced with permission from Ref. [85]. Copyright 2016, Wiley-VCH. **c** Representation of the preparation of N, P-doped graphene. **d**, **e** OER polarization curves and Tafel plots of N, P-doped graphene. **c**–**e** Reproduced with permission from Ref. [87]. Copyright 2015, American Chemical Society

remarkable OER performance due to the balanced composition and synergistic effect of heteroatoms. Above discussions enlightened the importance of heteroatom doping with the multiple effective synthetic approaches for optimizing the OER performances of 2D heteroatom-doped graphene-based electrocatalysts. The modified graphene-based materials by using single as well as multiple heteroatom doping strategy could possess excellent surface characteristics and more exposed active sites, which may further increase their OER activities and show the potential to be used as the substitutes of noble metal-based electrocatalysts.

Heteroatom-doped graphene-based electrocatalysts for overall water splitting

Recent developments have revealed the outstanding potentials of some emerging 2D heteroatom-doped graphene electrocatalysts to perform overall water splitting owing to the good intrinsic properties, including rapid electron transfer and high durability. The above discussions indicated that the 2D modified graphene-based electrocatalysts not only show excellent catalytic performances to conduct HER and OER, but also demonstrate their potentials for HER and OER in a same electrolytic cell. Accordingly, an efficient bifunctional metal-free catalyst contained N, F co-doped graphene nanosheets (NFGNs) was designed by using a simple chemical etching method for overall water splitting (Fig. 4a–c) [90]. The configurations with rich pyridinic N doping were found effective to conduct electrochemical process. Electrochemical performances demonstrated that the NFGNs attained the overpotential of 0.33 V during HER process, and the overpotential of ~ 0.34 V during OER process to reach up to the current density of 10 mA cm^{-2}. Moreover, the NFGNs electrocatalyst acquired the potential of ~ 1.90 V to gain the 10 mA cm^{-2} during overall water splitting in alkaline electrolyte, which was analogous to Pt/C bifunctional electrocatalyst (Fig. 4d). Density functional theory (DFT) calculations provided more understanding about the high activity of the NFGNs. It was revealed that the existence of synergistic effect between N and F heteroatoms enabled the heteroatom-doped graphene to alter the electron-withdrawing and electron-donating capabilities of carbon. Therefore, the electronic structure of NFGNs was found favorable to alter the carbon sites around the heteroatoms, which indicated the origin of the high electrochemical activities to demonstrate overall water splitting. Subsequently, the N, S-doped graphitic sheets (SHG) equipped with bifunctional properties were fabricated via annealing treatment of melamine-nickel sulfate complex, and potassium chloride at 900 °C for water splitting (Fig. 5a–c) [91]. The SHG catalyst performed excellent HER and OER in basic electrolyte with the Tafel slopes of 112 and 71 mV dec^{-1}, respectively. In addition, the SHG showed good potential to be used as both electrodes and reached the 10 mA cm^{-2} with a reasonable potential of 1.70 V and good stability in 1.0 M KOH during overall water splitting. Moreover, likewise Pt/C and RuO_2 setup, the SHG displayed an onset potential of 0.25 V, which was gradually increased with increasing current density during overall water splitting (Fig. 5d–h). The admirable electrochemical performances of SHG electrocatalyst was devised from the synergistic effect between unique structured SHG and the presence of heteroatom N, S dopants.

Besides N, F and N, S multi heteroatom-doping, the bifunctional electrocatalysts with N, O co-dopants have been also explored for overall water splitting. For instance, a novel catalyst composed of N, O co-doped graphene nanorings-integrated boxes (NOGB) was prepared by using pyrolysis of polydopamine and Prussian blue at 800 °C [92]. The NOGB prepared at 800 °C exhibited impressive bifunctional activities in an electrolytic cell by achieving the current density with 10 mA cm^{-2} with a considerable potential of 1.65 V in basic solution, which was marginally smaller than SHG (1.70 V) (Fig. 5e, f) [91]. It was revealed that the enhancement in the catalytic activity was accredited to the multi-atom (N, O) doping because these dopants might enhance the formation of carbon (C^+) active sites, which led to the enhanced electrochemical activity. To conclude, the heteroatom doping of graphene might provide the synergistic effect and modify the electronic structure, leading to abundant carbon active sites, which led to the desirable electrochemical overall water splitting performances.

2D porous carbon-based electrocatalysts for water splitting

Heteroatom-doped graphene based electrocatalysts have shown impressive applications for electrochemical water splitting, while their low porosity and limited surface area motivated the researchers to explore 2D porous carbon-based electrocatalysts with high porous structures and novel physicochemical properties. Recently, 2D porous carbon-based materials, including heteroatom-doped mesoporous carbons, N-doped hierarchically porous carbon nanosheets (NHPCNs), 2D porous carbons with structural defects, co-doped PCNs, and transition metals with heteroatom co-doped porous carbons have received wide spread consideration by virtues of their large surface areas and high porosity, which may lead to promising catalytic activities for various electrochemical applications including HER, OER, and overall water splitting [93–96].

2D porous carbon-based electrocatalysts for hydrogen evolution reaction

Current 2D porous carbons modified with heteroatom (N, S, and P) doping and/or transition metals doping have been broadly studied for HER owing to their porous structures, large surface areas, easy modifications, and abundant active sites [97, 98]. Moreover, the doping of heteroatom into carbon skeleton could cause dramatic impacts on charge distribution and electron modulation, which could enhance the electrochemical performances for HER [31, 99, 100]. For instance, a N-doped ordered mesoporous carbon (NOMC) was developed

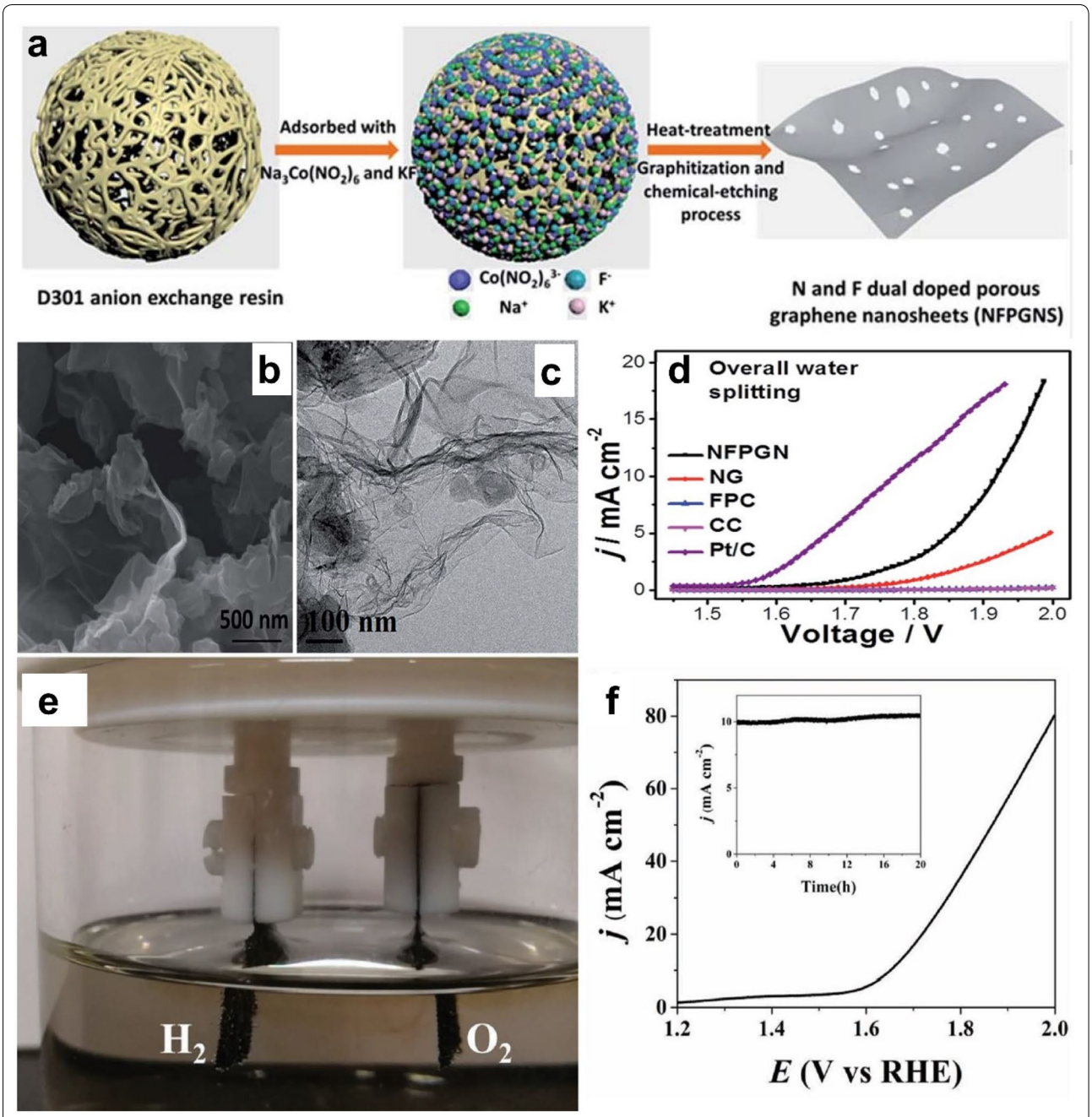

Fig. 4 **a** Synthetic routes of NFPGNS. **b**, **c** SEM images of NFGNS. **d** Steady-state curves of NFPGNS, NNG, FPGC, CC and Pt/C for overall water splitting in 1.0 M KOH. **a**–**d** Reproduced with permission from Ref. [90]. Copyright 2017, Royal Society of Chemistry. **e** The generation of gas bubbles during overall water splitting. **f** LSV curve of NOGB in 1 M KOH. The inset is representing the stability of the electrocatalyst in an electrolyser for 20 h. **e**, **f** Reproduced with permission from Ref. [92]. Copyright 2019, Wiley-VCH

by a pyrolysis treatment of carbon precursors at 900 °C [101]. The as-prepared NOMC catalyst presented a fair HER activity in basic solution and possessed a lower Tafel slope of 70 mV dec^{-1} than N-doped graphene (143 mV dec^{-1}) [75]. The N atoms were assisted as the active sites for HER, and the catalytic performance was considerably improved with the increased N content in NOMC.

Additionally, the introduction of multi heteroatoms (such as P, N and S, N) into carbon skeleton could also modulate electronic potential distribution and the electron density in the porous carbon matrix, offering the

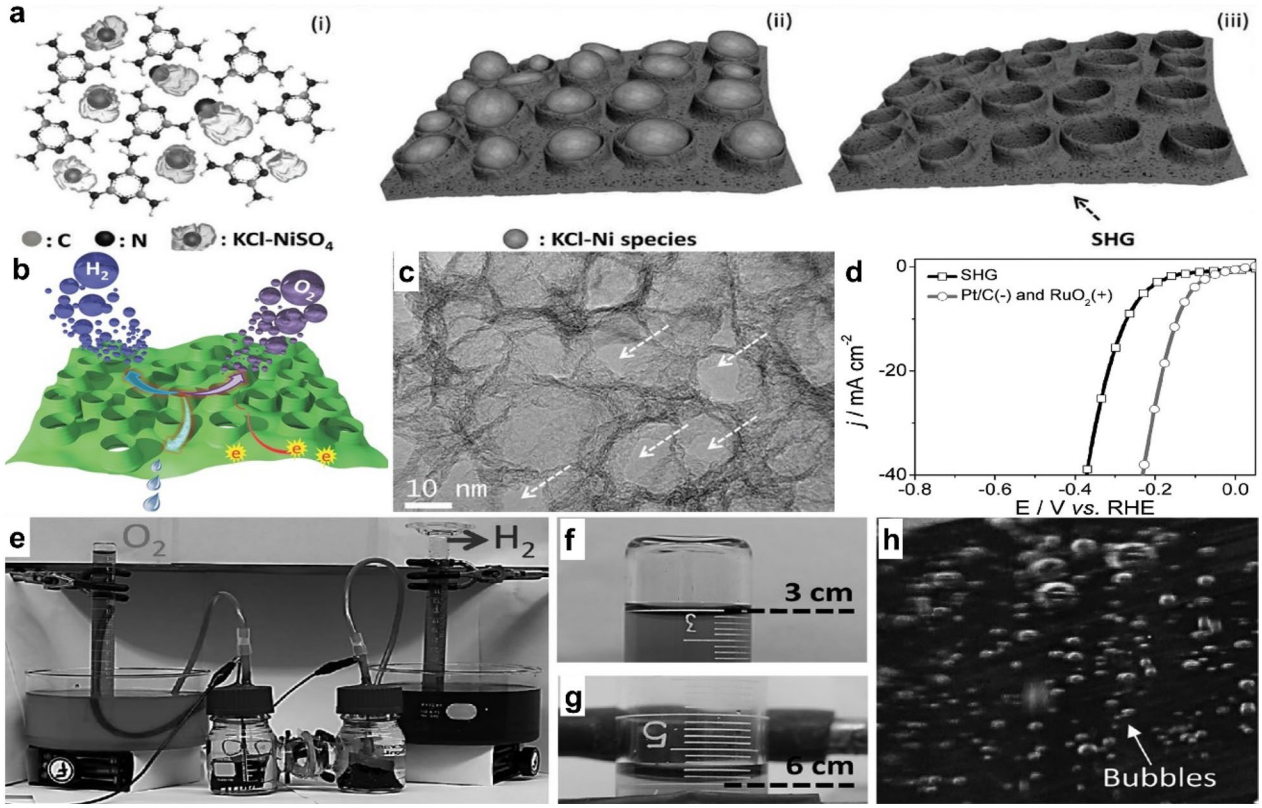

Fig. 5 **a** Synthetic process of SHG. (i) Powder of mixed melamine and nickel sulfate complex with KCl by ball milling. (ii) Structure of 2D Ni-KCl@SHG in situ grown from Ni@KCl and KCl seeds after annealing treatment. (iii) Well-defined structure of SHG after etching with the Ni@KCl and KCl seeds, followed by additional annealing treat. **b** Schematic representation of SHG. **c** Scanning electron microscopy (SEM) image of SHG. **d** Polarizations curves of SHG during overall water splitting. **e** Overall water slitting demonstration of SHG in a two-electrode water splitting device by chronopotentiometry at a given potential of 2 V. **f** O_2 and **g** H_2 collection process with displacement of water. **h** Bubbles generated during the overall water splitting process. **a**–**h** Reproduced with permission from Ref. [91]. Copyright 2016, Wiley-VCH

favorable active sites for the adsorption of H*, which can remarkably increase the electrocatalytic performance of 2D porous carbon-based electrocatalysts for HER [75, 102–104]. Recently, a mesoporous carbon with dual-doping of N and P atoms obtained from bacterium strain with large surface area of 816 $m^2\ g^{-1}$ was developed by a carbonization method at 900 °C (Fig. 6a) [105]. The as-prepared N, P dual-doped mesoporous carbon represented a smaller Tafel slope of 58.4 mV dec^{-1}, as well as lower overpotential of ~ 0.21 V to attained the 10 mA cm^{-2} for the HER than the electrocatalyst without mesoporous structure (88 mV dec^{-1} and ~ 0.42 V) in acidic electrolyte (Fig. 6b). The occurrence of N and P co-dopants on mesoporous carbon surface provided a strong synergistic effect, which was associated to the remarkable HER activity. Similarly, S, N co-doped PCNs possessing surface area of 513.3 $m^2\ g^{-1}$ with high porosity were designed by calcination treatment of sucrose, sulfur powder, and $MgCl_2$ under various temperatures from 600 to 900 °C [106]. The S, N-doped carbon synthesized at 800 °C suggested a decent HER electrochemical activity in acidic electrolyte, yielding a Tafel slope of 67.8 mV dec^{-1} along with a marginally high overpotential of ~ 0.12 V, as compared to Pt/C (31 mV) at 10 mA cm^{-2} (Fig. 6d). Conclusively, the S and N dopants considerably altered the electronic structures of graphene, providing the stronger interaction with H^+ than carbon atom, which enhanced the adsorption of hydrogen and upheld the HER activity (Fig. 6c). In another study, the S, N co-doped PCNs possessing high surface area of 830 $m^2\ g^{-1}$ were produced through annealing treatment of hair from 600 to 900 °C, followed by an activating agent of $ZnCl_2$ to produce large pores [107]. Notably, the S, N co-doped PCNs prepared at the annealing temperature of 800 °C exhibited excellent catalytic HER performance in acidic solution, which exhibited a Tafel slope of 57.4 mV dec^{-1}. In contrast, the other S, N co-doped PCNs prepared at 700 and 900 °C demonstrated the higher Tafel slopes, which were noted as 103.3 and 84.1 mV dec^{-1} in acidic electrolyte, respectively. Moreover, the S, N co-doped PCNs prepared at

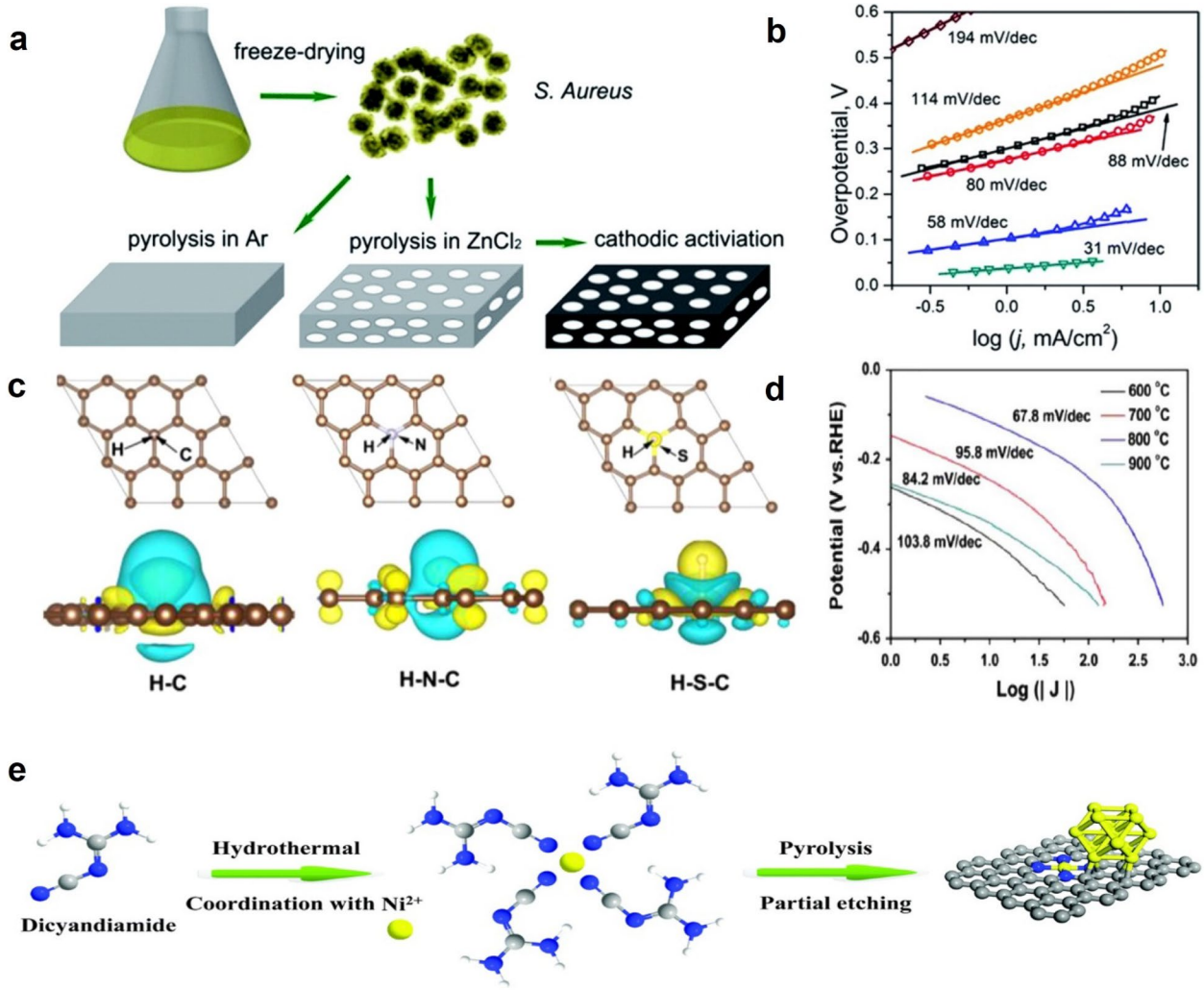

Fig. 6 **a** Representation of the synthetic procedure of the porous carbon and corresponding. **b** LSV curves. **a**, **b** Reproduced with permission from Ref. [105]. Copyright 2015, Royal Society of Chemistry. **c** Structural models and charge density of H adsorbed on the surface of carbon. **d** Corresponding Tafel plots of N, S-doped porous carbons. **c**, **d** Reproduced with permission from Ref. [106]. Copyright 2016, Elsevier. **e** Schematic of the synthetic route of Ni–N–C. Reproduced with permission from Ref. [108]. Copyright 2018, Wiley-VCH

800 °C demonstrated a reasonable small overpotential of 97 mV to gain the 10 mA cm^{-2}. Conclusively, the occurrence of C–S–C moieties and N-dopants in carbon matrix provided synergistic interaction, which contributed to the remarkable HER performances.

Besides heteroatom doping, the introduction of transition metal into carbon have been also explored due to their excellent charge polarizations and tunable electronic structures, which may lead to excellent HER performances. For instance, a novel Ni–N–C electrocatalyst composed of Ni–N_x attached on porous carbon embedded with Ni metal atoms was fabricated by using hydrothermal method, followed by simple pyrolysis of Ni ions and dicyandiamide at 900 °C for HER (Fig. 6e) [108]. The Ni–N-C demonstrated outstanding HER catalytic ability featuring a smaller Tafel slope of 183 mV dec^{-1}, along with lower overpotential of ~ 0.33 V than Ni nanoparticles (NPs) with exfoliated graphene (230 mV dec^{-1} and ~ 0.39 V) to acquire the 10 mA cm^{-2}. Conclusively, the Ni–N_x might easily decrease the energy barriers in dissociation of water molecules, which contributed to the satisfactory HER catalytic activity of Ni–N-C. In conclusion, the significant HER performances of 2D porous carbon-based electrocatalysts are associated to their high porosity, synergistic effect between porous carbons and transition metal and/or heteroatom dopants, large

surface area, and promising mass transport. Notably, these electrocatalysts could be readily developed on a large scale to catalyze HER.

2D porous carbon-based electrocatalysts for oxygen evolution reaction

According to scientific research, the 2D porous carbons have been found to be of great potential in OER, owing to their hierarchical pore, large surface area, and electrophilicity of carbon, which are capable of providing easy infiltration of electrolytes, absorption of OH^-, and rapid emission of O_2 after the combination of two adsorbed oxygen atoms [109–111]. For instance, the defect rich carbon nanosheets with ultrathin layered structure and exceptionally largest surface area of 1793 m^2 g^{-1} were constructed by carbonization of citric acid and NH_4Cl precursors at 1000 °C (Fig. 7a) [112]. During OER, the defect rich carbon nanosheets demonstrated a Tafel slope of 142 mV dec^{-1} in basic solution (Fig. 7c). Additionally, the defect rich carbon nanosheets showed potential of 1.64 V at 10 mA cm^{-2} and onset potential of 1.55 V, which were analogous to IrO_2 (1.59 and 1.48 V) (Fig. 7b).

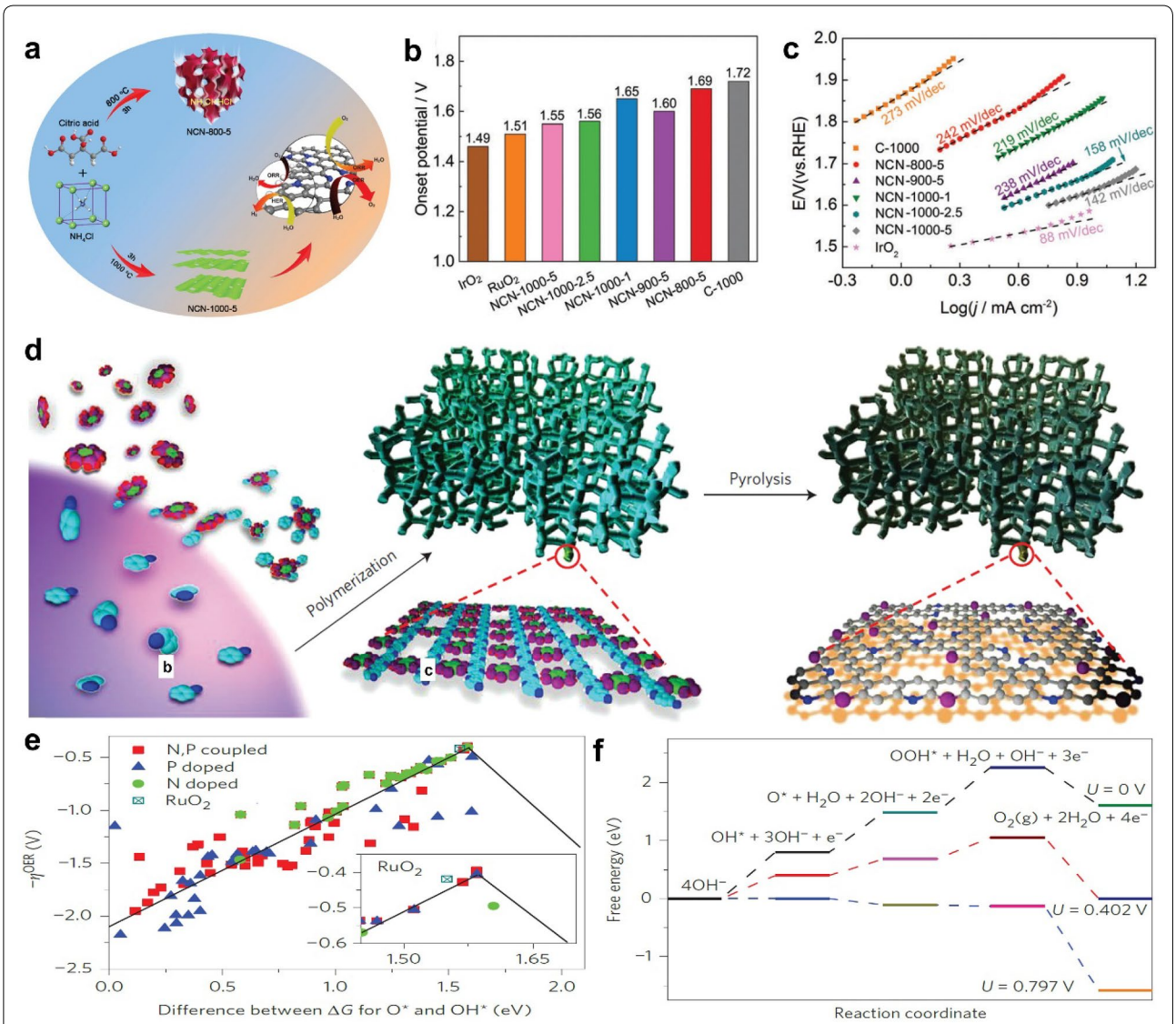

Fig. 7 **a** Illustration of the synthetic routes of N-doped porous carbon. Comparison of the **b** onset potentials and **c** Tafel slopes of N-doped porous carbon prepared at 1000 °C with other controlled samples. **a**–**c** Reproduced with permission from Ref. [112]. Copyright 2019, Royal Society of Chemistry. **d** Schematic representation of synthesis of NPMC foams. **e** The OER volcano plots correlating the overpotential versus adsorption energy of O* and the difference between the adsorption energy of O* and OH* for N-doped, P-doped, and N, P-doped graphene, respectively. **f** Free energy diagram for the OER pathway. **d**–**f** Reproduced with permission from Ref. [113]. Copyright 2015, Nature Publishing Group

The DFT calculations indicated that the porous structure with abundant carbon edge defects and N dopants was associated to impressive electrocatalytic activity of the defect rich carbon nanosheets.

As it is well established, co-doping with heteroatoms and high surface area of the 2D porous carbons can play effective roles in enhancing the adsorption ability and providing more exposed active sites. For example, N, P co-doped mesoporous carbons (NPMC) were fabricated by annealing treatment of PANI aerogels from 900 to 1100 °C (Fig. 7d), among which the largest surface area was 1663 m^2 g^{-1} for NPMC prepared at 1000 °C [113]. The electrochemical results indicated that the NPMC prepared at 1000 °C carried out a marginally low overpotential of 0.39 V at 10 mA cm^{-2}, which was comparatively smaller than single P-doped and N-doped mesoporous carbons (0.49 and 0.41 V), suggesting appreciable OER catalytic performance of the co-doped NPMC (Fig. 7e, f). The high OER performance of NPMC was originated from the highly porous structure of carbon and the N, P co-doping.

Despite of enormous improvements in the development of 2D porous carbon-based electrocatalysts, it is still challenging to improve their catalytic activities to compete with the noble metal-based electrocatalysts. It was noticed that the doping of small amount of transition metals accompanied with heteroatoms could be more beneficial towards the enhancement of electrochemical activities of electrocatalysts [114]. For example, a novel Co, N-doped carbon-based (Co-NMC) catalyst possessing a trace level of cobalt doping and large surface area of 540 m^2 g^{-1} was developed via adopting template based synthetic approach, followed by carbonization treatment of Co precursors, melamine, and g-C_3N_4 at 900 °C for OER [115]. The Co-NMC attained the 10 mA cm^{-2} at a much smaller overpotential of 0.35 V than the NMC (~ 0.50 V) in alkaline solution. The excellent conductivity, great mass transport, synergistic interaction between Co, N-doping and the existence of Co-N_x active sites resulted in high OER performance of the Co-NMC electrocatalyst. In another study, a novel OER electrocatalyst of Ni–N–S doped porous carbon was designed by annealing treatment of dicyanamide-thiophene-nickel salt at 900 °C (Fig. 8a–d) [116]. The Ni–N–S doped porous carbon displayed a considerably low Tafel slope of 45 mV dec^{-1}. While, acting as an OER electrocatalyst, the Ni–N–S doped porous carbon showed an overpotential of 1.51 V to attain the current density of 10 mA cm^{-2} (Fig. 8g). Moreover, the Ni–N–S doped porous carbon outperformed the well-established Ir/C electrocatalyst in basic electrolyte, which presented a high Tafel slope of 88 mV dec^{-1} (Fig. 8f). Conclusively, the well dispersed Ni–N–S species were acted as active sites, and provided the excellent electron transfer with promoted reaction kinetics, which enhanced the OER performance of Ni-N-S doped porous carbon (Fig. 8e). Notably, the 2D porous carbon-based electrocatalysts with heteroatoms and transition metal doping possess large surface area, promising mass transport, and mechanical robustness, which make them promising candidates for OER electrocatalysts.

2D porous carbon-based electrocatalysts for overall water splitting

Although 2D porous carbon-based electrocatalysts have exposed remarkable potential as single functional electrocatalysts for either HER or OER, it is still challenging to use them as bifunctional electrocatalysts to perform overall water splitting with admirable durability. Accordingly, 2D porous carbons with the structure defects and heteroatom dopants were used as highly stable and economical electrocatalysts to conduct overall water splitting, by virtue of outstanding characteristics, such as low cost, strong tolerance to harsh acidic or basic conditions, fast electron transfer, large surface area. In this regard, a metal-free defect-rich porous carbon (DRPC) bifunctional electrocatalyst having a large surface area of 1811 m^2 g^{-1} was developed by polymerization reaction, followed by the pyrolysis of polymerized product at 900 °C to demonstrate the overall water splitting (Fig. 9a, b) [117]. It was revealed that the DRPC accompanied immense N-content of 9.3 at % and displayed excellent bifunctional catalytic performances in alkaline media for both HER and OER. Importantly, during overall water splitting, the DRPC electrocatalyst demonstrated a low voltage of 1.74 V at the 10 mA cm^{-2} with high stability, which was considerably lower than porous carbon (2.11 V), and slightly higher than Pt/C//RuO_2 (1.66 V) (Fig. 9c, d). The edge defects, large surface area, and high N-doping content were attributed to the remarkable electrochemical performances. Subsequently, a N-doped carbon-based electrocatalyst with largest surface area of 1017 m^2 g^{-1}, was developed by cathodic polarization treatment (CPT) for different time after pyrolysis of different precursors [118]. The N-doped carbon-based electrocatalysts prepared by using CPT for 6 h and 4 h demonstrated impressive HER and OER activities, with the overpotentials of ~ 0.16 and ~ 0.48 V at 10 mA cm^{-2}, and Tafel slopes of 54.7 and 78.5 mV dec^{-1} in acidic media, respectively. Additionally, in two-electrode water system, the two N-doped carbon-based electrocatalysts by using CPT for 6 h and 4 h achieved the current density of 10 mA cm^{-2} with the minimum voltage of 1.82 V, which was smaller than porous carbon-based counterparts (~ 2.0 V) in 0.1 M KOH [117]. The tremendous

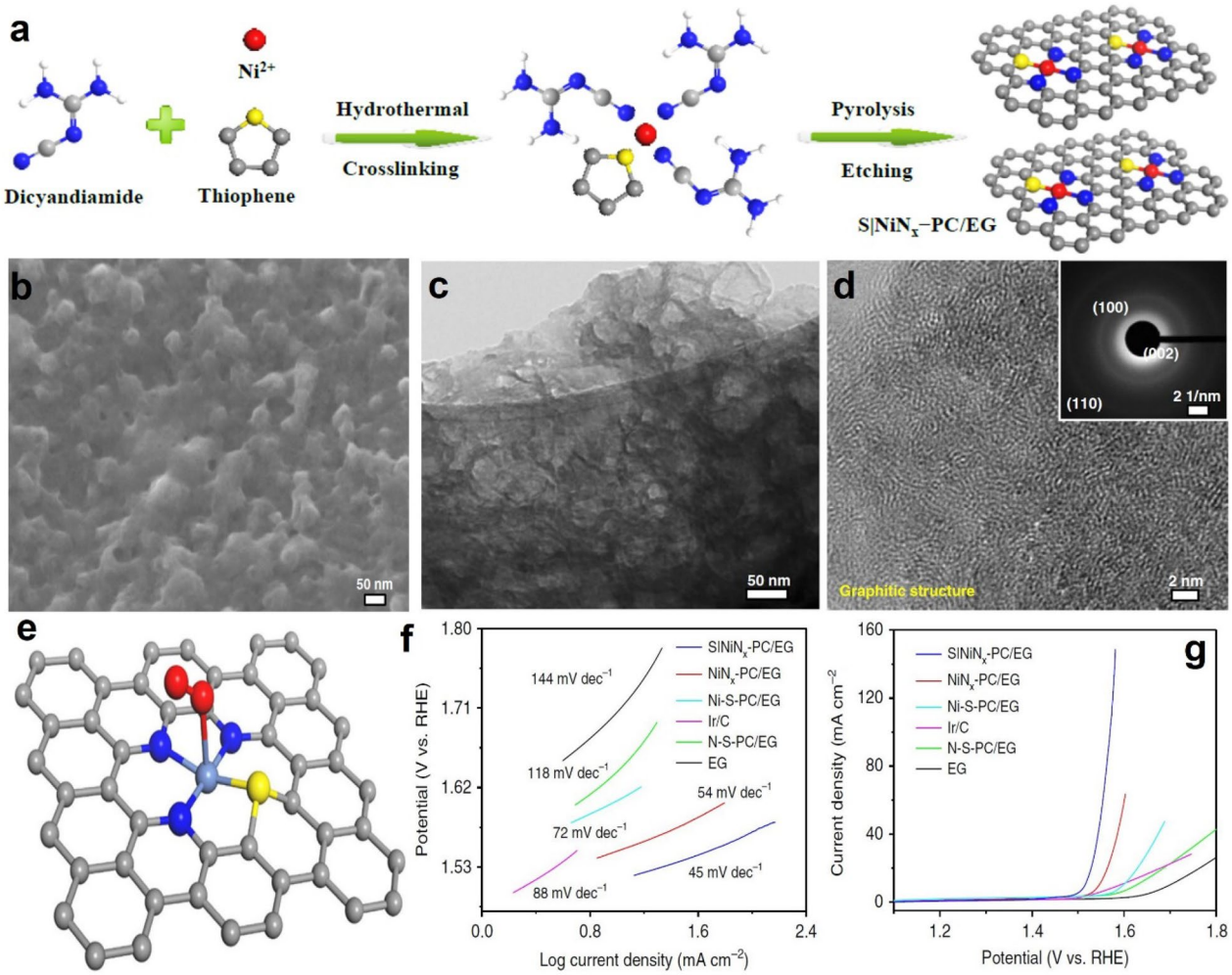

Fig. 8 **a** Schematic of the synthetic route of Ni–N–S doped porous carbon. **b** SEM. **c** TEM image. **d** HRTEM and inset of C is the SAED pattern. **e** Representation of structural model of Ni–N–S doped porous carbon. **f**, **g** Electrochemical performances of Ni–N–S doped porous carbon with other control samples. **a**–**g** Reproduced with permission from Ref. [116]. Copyright 2019, Nature Publishing Group

overall water splitting activity of N-doped carbon-based electrocatalyst might be ascribed to the composition of functional groups attained by using CPT for different reaction time. Moreover, the CPT altered the configuration of functional groups of the precursors without destroying the large surface area and the porosity.

Based on the above discussion, 2D porous carbon-based catalysts have exhibited the high catalytic efficiencies owing to their unique advantages, including high porosity, large surface area, and fast mass transportation, which thereby may lead to the enhanced overall water splitting performance. Furthermore, the advancement in the field of 2D porous carbon-based electrocatalysts underpins the further research for the novel and scalable production of noble metal-free 2D carbon-based electrocatalysts to conduct overall water splitting with high efficiencies.

2D carbon-based hybrid electrocatalysts for water splitting

Significant attempts have been exercised to develop 2D carbon-based hybrids, including 2D nanocarbons with transition metal compounds and metal-free g-C_3N_4 for water splitting. The integration of transition metal compounds, such as transition metal sulfides, oxides, and phosphides or metal-free materials including g-C_3N_4 and exfoliated black phosphorus (EBP) with carbon skeleton provides abundant catalytic active sites, while the carbon supports prevent the aggregation of transition metal compounds or metal-free substances, and provide high conductivity, which can enhance electrocatalytic activities of 2D carbon-based hybrids towards HER, OER, and overall water splitting [119–127].

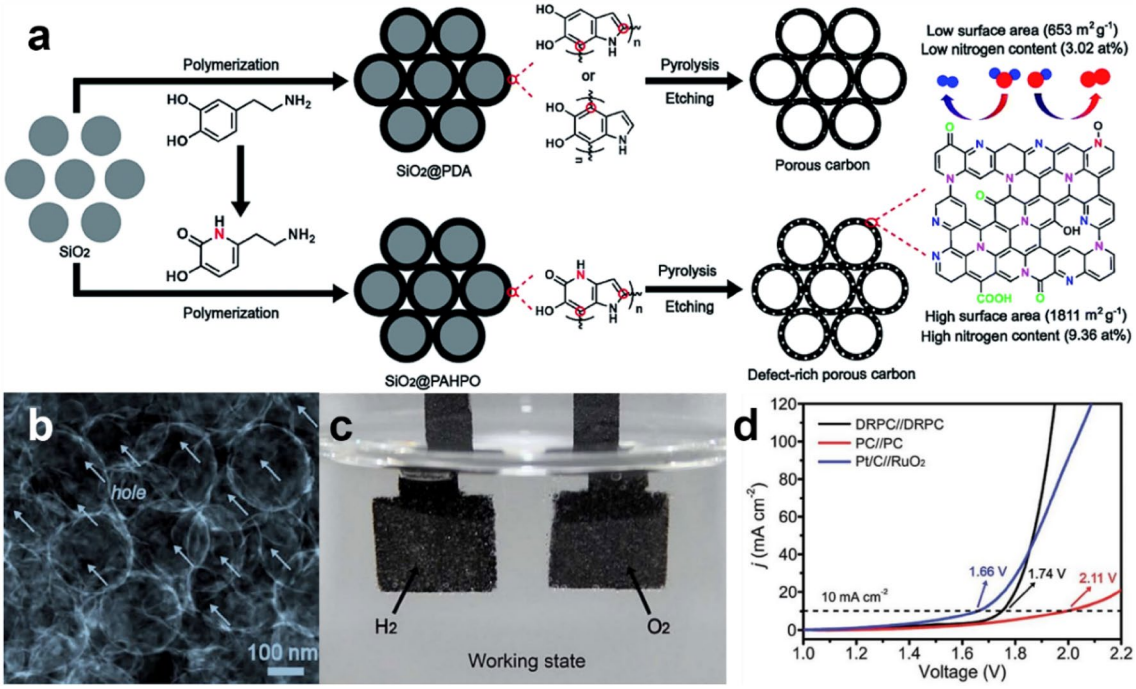

Fig. 9 **a** Representation of synthetic route of DRPC. **b** STEM image of DRPC. **c** Evolution of bubbles from DRPC electrodes during overall water splitting. **d** Polarization curves of DRPC. **a**–**d** Reproduced with permission from Ref. [117]. Copyright 2017, Royal Society of Chemistry

2D carbon-based hybrid electrocatalysts for hydrogen evolution reaction

Recently, 2D carbon-based hybrids including modified graphene with transition metal sulfides and phosphides have attained enormous attention owing to the benefits of transition metal compounds which act as catalytic active sites and 2D nanocarbons which provide high dispersion of active sites with high conductivity, leading to the improved HER performances. Among these transition metal compounds, bulk molybdenum disulfide (MoS_2) is electrochemically inert for HER, whereas synthetically developed nanostructured MoS_2 electrocatalysts have gained much consideration due to their earth abundance and more exposed edges, which can result in impressive catalytic performance for HER [128]. For example, a MoS_2/rGO hybrid with abundant exposed active sites was prepared by a solvothermal method, which was found to be an effective strategy in preventing the aggregation of MoS_2 NPs [128]. The MoS_2/rGO hybrid showed impressive electrocatalytic activity towards HER, featuring by a smaller Tafel slope of 41 mV dec^{-1} than that of the pure MoS_2 NPs (94 mV dec^{-1}) in acidic condition. Moreover, the MoS_2/rGO hybrid reached up to 10 mA cm^{-2} at the potential of ~ 0.15 V. The impressive HER property of MoS_2/rGO hybrid was originated from the strong coupling effect between MoS_2 and rGO sheets, and highly dispersed catalytic active sites. Other than transition metal sulfides, a transition metal phosphide based electrocatalyst consisting of iron phosphide (FeP) and graphene sheets was developed by using thermal treatment of Fe_3O_4, GO, and tetraethylene glycol at 180 °C, followed by phosphidation treatment at 350 °C for HER [129]. Well-structured FeP/graphene hybrid presented an admirable HER electrocatalytic activity with an overpotential of 123 mV to attain the 10 mA cm^{-2} in 0.5 M H_2SO_4. Moreover, the FeP/graphene hybrid exhibited lower Tafel slope of 50 mV dec^{-1} compared to the FeP NPs (67 mV dec^{-1}). Conclusively, the synergistic effect between FeP NPs with rich active sites and conductive graphene supports led to the outstanding electrochemical activity of the FeP@graphene hybrid. Apart from FeP, other transition metal phosphides have also been hybridized with 2D nanocarbons to explore their electrochemical activity for water splitting. For example, a unique electrocatalyst composed of N-doped reduced graphene oxide (NRGO) and Ni_2P NPs was fabricated by an in situ thermal decomposition strategy for HER [130]. The Ni_2P/NRGO hybrid showed excellent HER performances, featuring by a smaller Tafel slope of 59 mV dec^{-1} than Ni_2P/rGO (105 mV dec^{-1}). In addition, further electrochemical measurements revealed that the Ni_2P/NRGO hybrid required a smaller overpotential of 0.10 V to obtain the current density of 10 mA cm^{-2} than the Ni_2P/rGO (~ 0.36 V). The as-prepared Ni_2P/NRGO

hybrid possessed admirable conductivity, the charged natures of P and Ni, and the synergistic interaction between Ni_2P NPs and NRGO, which contributed to the enhanced the HER performance.

Besides transition metal-based hybrids, 2D carbon-based hybrids with metal-free g-C_3N_4 have also showed great capability to replace noble metal-based electrocatalysts for HER, due to their novel characteristics including high N-content of metal-free g-C_3N_4, favorable conductivity of carbon support, rapid electron transfer, and excellent stability against oxidation [131]. In this regard, a metal-free hybrid composed of g-C_3N_4 and N-doped graphene (C_3N_4@NG) was constructed via annealing treatment of GO and dicyandiamide at 600 °C to conduct HER when adopting acidic and alkaline electrolytes [132]. The C_3N_4@NG hybrid demonstrated a Tafel slope of 51.5 mV dec^{-1}, indicating superior HER activities in acidic solution. Also, the C_3N_4@NG hybrid required a lower overpotential of 0.24 V than NG (~0.55 V) to reach up to 10 mA cm^{-2}. Impressively, the synergistic effect between conductive NG and g-C_3N_4 upheld the promising HER performance of C_3N_4@NG hybrid. Specifically, the DFT calculations revealed that the integration of metal-free g-C_3N_4 with NG caused the charge density in hybrid, promoting electron transfer between NG and metal-free g-C_3N_4, which were found beneficial for the improved HER property of C_3N_4@NG. Additionally, a metal-free 2D hybrid consisting of P-doped graphene and g-C_3N_4 was constructed by a thermal exfoliation of triphenylphosphine and dicyandiamide [133]. The designed hybrid catalyst represented a Tafel slope of 90 mV dec^{-1}, indicating appreciable HER activity in acidic media. In the meantime, the hybrid displayed a small overpotential of 0.34 V to obtain the 10 mA cm^{-2} during HER. However, the individual P-doped graphene attained the higher overpotential of ~0.40 V under the current density of 10 mA cm^{-2}. More evidences indicated that strong coupling effect of P-doped graphene with g-C_3N_4 provided strong synergistic effect in the graphene matrix, which contributed to the excellent HER activity. It is note-worthy that the integration of 2D nanocarbons with transition metal compounds or metal-free g-C_3N_4 provided the unique properties in terms of good conductivity from carbon supports and high accessible catalytic active sites from transition metal compounds and metal-free g-C_3N_4 to the 2D carbon-based hybrids, which were found beneficial to demonstrate excellent HER performances.

2D carbon-based hybrid electrocatalysts for oxygen evolution reaction

From the last decade, enormous attempts have been exercised to develop 2D carbon-based hybrids with transition metal compounds for OER, due to the abundant active sites of transition metal compounds, high conductivity of carbon supports, and rapid electron transfer between them, which could be the key parameters in the improvement of electrochemical activities of such hybrids [134–137]. For instance, a novel CoP_2/rGO electrocatalyst composed of CoP_2 NPs and rGO sheets was synthesized by thermal treatment of GO, cobalt salt, and NaH_2PO_2 at 600 °C for OER [138]. As-prepared CoP_2/rGO electrocatalyst presented a lower Tafel slope of 96 mV dec^{-1} than bulk CoP_2 (103 mV dec^{-1}), indicating the remarkable OER activity of the CoP_2/rGO in 1.0 M KOH. Moreover, further electrochemical measurements revealed that the overpotential of CoP_2/rGO was 0.30 V, which was also lower than the bulk CoP_2 (0.37 V) to reach up to 10 mA cm^{-2}. Decisively, the small size CoP_2 NPs on rGO was acted as active sites, which might be responsible for the remarkable activity of CoP_2/rGO to conduct OER. Additionally, the OER electrocatalysts composed of S, N co-doped porous graphene sheets (SNGS) with Co/Co_9S_8 were fabricated by using pyrolysis treatment of GO, cobalt nitrate, and thiophene-2,5-dicarboxylate precursors from 800 to 1100 °C [139]. The Co/Co_9S_8@SNGS hybrid prepared at 1000 °C demonstrated outstanding OER performance in 0.1 M KOH with an overpotential of 0.29 V at 10 mA cm^{-2}. Meanwhile, the Co/Co_9S_8@SNGS displayed a smaller Tafel slope of ~80 mV dec^{-1} than RuO_2 (~129 mV dec^{-1}), indicating the superior OER activity of the hybrid. The exceptional OER catalytic performance was associated to the synergistic effect of SNGS and Co/Co_9S_8, as well as the porous structure of Co/Co_9S_8@SNGS.

Other than transition metal compounds hybrids, the 2D nanocarbons with metal-free g-C_3N_4 and other materials have also been investigated to conduct OER [140, 141]. For instance, a novel metal-free hybrid consisting of an ultrathin g-C_3N_4 nanosheets and graphene was explored as efficient OER electrocatalyst, which was designed by pyrolysis treatment of GO and melamine at 600 °C, followed by ultra-sonication [142]. The g-C_3N_4@graphene hybrid represented an onset potential of 0.58 V with a larger anodic current density than individual graphene and g-C_3N_4 nanosheets. Moreover, the g-C_3N_4@graphene hybrid demonstrated a Tafel slope of 68.5 mV dec^{-1}, which was considerably smaller than the g-C_3N_4 nanosheets (120 mV dec^{-1}) in alkaline electrolyte. In addition, further comparison of OER performance of the hybrid was made in terms of potential, and the results confirmed that the g-C_3N_4@graphene hybrid required a lower potential of ~0.80 V than g-C_3N_4 nanosheets (~0.97 V) to reach the 10 mA cm^{-2}. Decisively, the high OER electrochemical property of g-C_3N_4@graphene hybrid was ascribed to the integration

of graphene and ultrathin g-C_3N_4 nanosheets with pyridinic N related active sites. In another study, an efficient metal-free hybrid composed of N-doped graphene and CNTs with high surface area of 812.9 m^2 g^{-1} was synthesized by using high temperature chemical vapor deposition (CVD) method at 950 °C [30]. The N-doped graphene/CNTs (NGSH) hybrid demonstrated excellent OER performance with the potential of 1.63 V at the current density of 10 mA cm^{-2}, which was analogous to IrO_2/C (~ 1.60 V) [109]. In addition, the NGSH showed an exceptionally smaller Tafel slope of 83 mV dec^{-1} than commercial Pt/C (288 mV dec^{-1}), suggesting remarkable OER activity of the NGSH hybrid in 0.1 M KOH. The high performance of the NSGH hybrid was attributed to the N-doping, large surface area, high graphitic degree, and abundant porosity. Convincingly, the excellent OER performance of the 2D carbon-based hybrids was proposed due to the good electronic contact and efficient electron transfer between 2D nanocarbons and transition metal compounds/metal-free materials, which make them potentially low cost substitutes to noble metal-based electrocatalysts for OER applications.

2D carbon-based hybrid electrocatalysts for overall water splitting

Recently, 2D carbon-based hybrids with transition metal compounds have been widely employed as exciting electrocatalysts for overall water splitting owing to the combined advantages of transition metal compounds and 2D carbon supports, low cost, earth abundance, good stabilities, and promising electrocatalytic activities [143–148]. For instance, a highly efficient hybrid electrocatalyst composed of CoP and rGO sheets was synthesized by using simple pyrolysis of different precursors at 300 °C along with phosphating treatment [145]. The CoP/rGO hybrid with sheet-like morphology displayed admirable catalytic activity as both anode and cathode in terms of a small Tafel slope and low overpotential at 10 mA cm^{-2}, which were 135 mV dec^{-1} and 0.47 V, respectively. In contrast, the Pt/C as both anode and cathode demonstrated inferior performance by displaying a high Tafel slope of 251 mV dec^{-1}, as well as a high overpotential of 0.60 V to gain the 10 mA cm^{-2}. Accordingly, the remarkable overall water splitting activity of CoP/rGO hybrid was accredited to the synergistic effect of CoP and rGO. In another study, a hybrid consisting of the CoP NPs and P, N co-doped mesoporous graphene-like carbon (CoP@NPMG) was developed by crosslinking of phytic acid and melamine, followed by the pyrolysis treatment at 900 °C (Fig. 10a) [149]. When acted as both anode and cathode in basic media, the CoP@NMPG electrocatalyst yielded the considerable potential of ~ 1.6 V to attain the current density of 10 mA cm^{-2}, which was analogous to that of Pt/C//RuO_2 (1.56 V at 10 mA cm^{-2}). An electron transfer might occur between CoP NPs and N, P co-doped carbon, and the carbon atoms between N and P atoms in the carbon layers turned into active sites, which led to the high electrochemical performances of CoP@NPMG.

Besides CoP, the cobalt oxides were also captivated extensive consideration owing to their decent catalytic activity [150]. A cobalt–cobalt oxide with N-doped carbon-based electrocatalyst (CoO_x@CN) was designed by using a one-pot thermal treatment of cobalt salt, melamine, and glucosamine hydrochloride at 800 °C (Fig. 10b) [151]. The as-synthesized CoO_x@CN showed a good activity during overall water splitting in alkaline electrolyzer. When acted as both anode and cathode, the CoO_x@CN hybrid attained ~ 20 mA cm^{-2} at a voltage of 1.55 V, which was almost analogous to other reported transition metal-based electrolytic cell composed of NiO/Ni-CNT and Ni–Fe layered double hydroxide (LDH) (1.50 V at 20 mA cm^{-2}) (Fig. 10c, d) [152]. Structural characterization indicated that the high catalytic activities of as-prepared CoO_x@CN were linked to the synergistic effect between CoO and Co, promising conductivity of N-doped carbon, and the presence of electron rich N atoms. A bifunctional electrocatalyst based on iron oxyhydroxide/nitride (FeOOH/FeN_4) and vertically aligned carbon nanosheets (VCNs) was fabricated by a template method, followed by pyrolysis of VCNs and iron-based precursors at 500 °C to conduct overall water splitting [153]. Acting as an OER electrocatalyst, the VCNs@FeOOH displayed an overpotential of ~ 0.18 V at 10 mA cm^{-2}. In contrast, the VCNs@Fe_4N demonstrated excellent HER with an overpotential of 0.17 V at 10 mA cm^{-2}. When the VCNs@FeOOH employed as anode and VCNs@Fe_4N served as cathode in a full electrolytic cell, the bifunctional electrocatalysts exhibited a potential of 1.60 V under the current density of 10 mA cm^{-2}, which was comparable to Ni–Fe LDH (1.70 V) and FeMnP (1.60 V) [154, 155]. The VCNs@Fe_4N//VCNs@FeOOH bifunctional electrocatalysts delivered outstanding catalytic performance with excellent stability due to their accelerated electron transfer, mass transport ability, the synergistic effect of multiple components, and exposed active sites. In another study, a hybrid catalyst by coupling of defective graphene with exfoliated Ni–Fe LDH nanosheets (LDH-NS) was developed for overall water splitting (Fig. 10e) [156]. This hybrid, acted as both cathode and anode, showed the lower potential of 1.50 V to obtain the current density of 20 mA cm^{-2} in basic solution than that of the CoO_x@CN couple (1.55 V) during overall water splitting (Fig. 10f-h) [151]. Convincingly, the strong interaction between LDH-NS and defective graphene provided a strong synergetic effect and rapid electron transfer, which might be

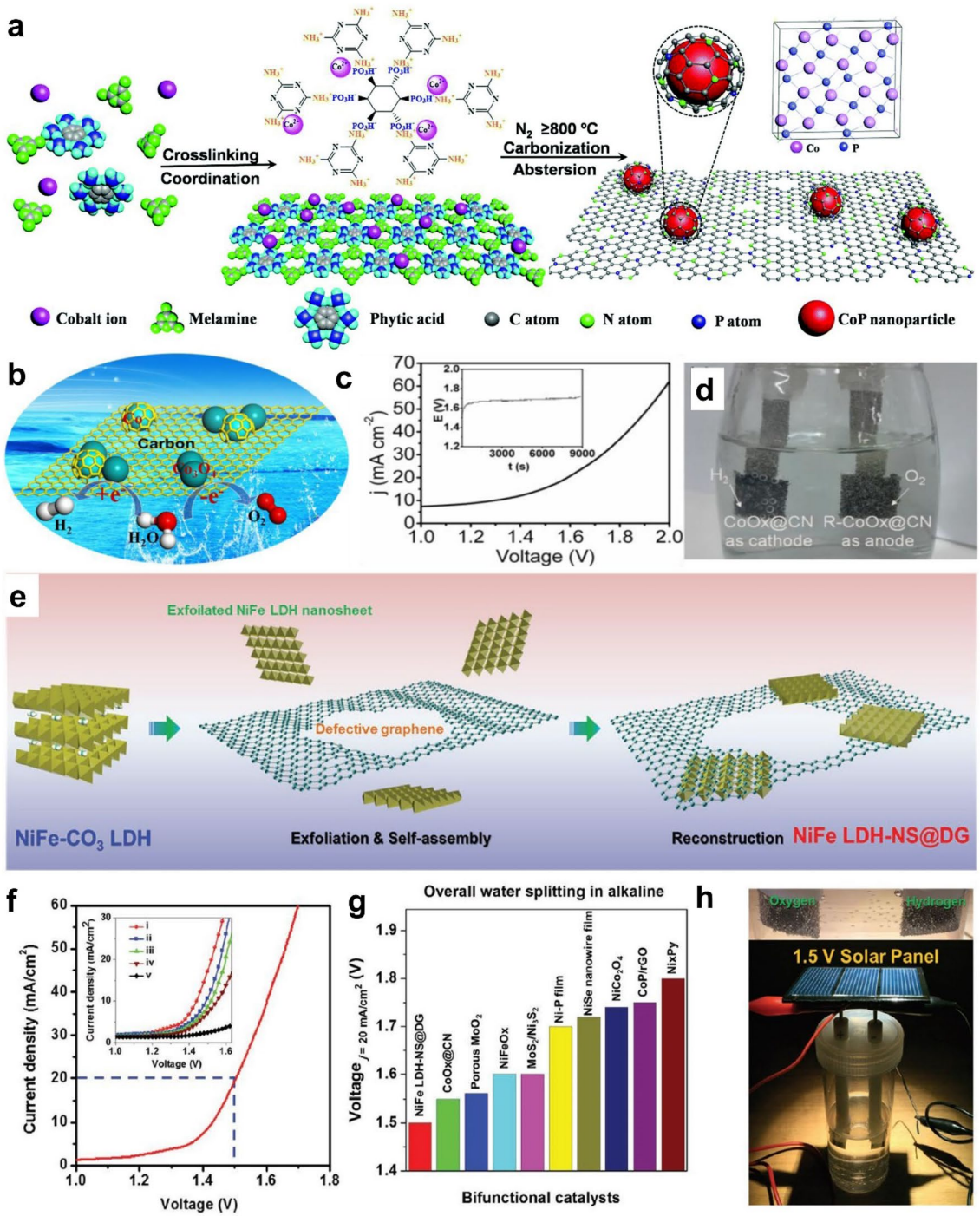

Fig. 10 **a** Illustration of the synthesis process of CoP@NPMG. Reproduced with permission from Ref. [149]. Copyright 2018, Royal Society of Chemistry. **b** Graphical representation of CoO_x@CN hybrid. **c**, **d** Corresponding polarization curve and generation of gas bubbles during over all water splitting. **b**–**d** Reproduced with permission from Ref. [151]. Copyright 2015, American Chemical Society. **e** Schematic representation of synthesis of NiFe LDH-NS@defective graphene. Electrochemical measurements of exfoliated graphene. **f** Polarization curve of NiFe LDH-NS@defective graphene as OER and HER catalysts in 1.0 M KOH for overall water splitting. **g** Comparison of NiFe LDH-NS@defective graphene catalyst with other benchmark noble metal-free bifunctional catalysts. **h** Demonstration of a solar power assisted water-splitting device with a voltage of 1.5 V. **e**–**h** Reproduced with permission from Ref. [156]. Copyright 2017, Wiley-VCH

the key factors to provide remarkable overall water splitting performance.

Besides transition metal compounds, the introduction of exfoliated black phosphorous (EBP) nanosheets has provided an opportunity to develop the metal-free hybrids for overall water splitting due to their unique properties including good carrier mobility of up to 1000 cm^2 V^{-1} s^{-1} [157–159]. For example, a novel hybrid consisting of EBP and N-doped graphene (EBP@NG) was prepared by sonication treatment, followed by the electrostatic interaction of EBP and NG [160]. The as-prepared EBP@NG hybrid achieved a current density of 10 mA cm^{-2} at the potential of 1.54 V in 1.0 M KOH for overall water splitting. In contrast, the Pt/C and RuO_2 couple in an electrolyzer showed a potential of 1.60 V at 10 mA cm^{-2}, which was higher than EBP@NG. The excellent performance of the EBP@NG hybrid was attributed to the unique heterostructure, leading to the effective electronic modulation, which enhanced the inherent catalytic abilities of EBP@NG hybrid. In conclusion, the above discussion revealed that the high overall water splitting activities of 2D carbon-based hybrids were originated from rapid electron transfer, mass transport ability, and the synergetic effect of 2D nanocarbons and transition metal compounds, which may enhance the widespread progress of efficient noble metal-free 2D carbon-based electrocatalysts in the same electrolyzer.

Conclusions

In this review, the recent advancements of noble metal-free 2D carbon-based electrocatalysts, and their promising electrochemical applications towards HER, OER, and overall water splitting were highlighted and discussed. The 2D carbon-based electrocatalysts, including heteroatom (B, N, S, P, F, and O) doped graphene, 2D porous carbons modified with transition metals and/or heteroatoms, 2D nanocarbons based transition metal compounds or metal-free hybrids were developed by adopting well-known synthetic methods, such as template method, hydrothermal method, CVD, pyrolysis, and CPT method, etc. These noble metal-free 2D carbon-based electrocatalysts possessed impressive characteristics, including excellent conductivity, affordable cost, large surface area, high porosity, abundant active sites, and good appreciable durability, which made them promising candidates to conduct HER, OER, and overall water splitting. Among mentioned 2D nanocarbons, the modification of graphene with high electronegative heteroatoms including single atom doping (B, S, and N) or multi-atom doping (N/S, N/P, N/O, and N/P/F) may alter the electronic structure of intrinsic graphene by converting the neighboring carbon atoms into active sites and boost the adsorption of reaction intermediates on the surface of modified graphene, which could enable electrocatalysts to effectively catalyze HER, OER, and overall water splitting. It was found that the dopants with higher (as N) or lower (as B) electronegativity than that of carbon, could create charged site (C^+), which is favorable for adsorption of catalytic intermediates including H*, O*, OH^-, and OOH^- to facilitate the water splitting process [7, 161]. Additionally, 2D porous carbon networks with heteroatom doping and/or transition metal doping possess large surface area, high porosity, outstanding mass transport, good mechanical stability, and easy functionalization for electrochemical reactions. Moreover, the high content of heteroatom doping in the porous carbons may induce local charge redistribution on adjacent carbon atoms by intramolecular charge transfer and provide good interaction with transition metal atoms, leading to the generation of intrinsic active sites, which may further enhance the electrocatalytic activities for water splitting [117, 160]. Last but not least, 2D nanocarbons with transition metal compounds and metal-free materials are used as effective electrocatalysts because of the unique advantages of transition metal compounds or metal-free substances that act as active sites as well as 2D carbon supports that could prevent aggregation of transition metal compounds, offer good dispersion of active sites and provide high conductivity. The presence of synergistic effect between 2D nanocarbons and transition metal compounds or metal-free materials with different adsorption abilities of H* could provide moderate adsorption–desorption behavior of H* and enhance OOH^* formation on their surfaces, which may lead to the enhanced water splitting performances [124].

Though noble metal-free 2D carbon-based electrocatalysts have presented great promises in HER, OER, and overall water splitting, the less durability and vulnerability for carbon corrosion under working conditions are certain limitations, which hinder their practical applications in devices such as rechargeable metal-air batteries and regenerative fuel cells [162, 163]. In addition, the 2D carbon nanosheets suffer from aggregation and overlapping or restacking due to intersheet van der Waals attractions as well as high surface energy, which may affect the properties of the individual sheet [94]. Anyway, there are still some grand challenges in the emerging field of noble metal-free 2D carbon-based materials as electrocatalysts for water splitting, which need to be overcome. First, the controllable fabrication of novel 2D carbon-based electrocatalysts with tunable morphologies and electronic structures are extremely important to achieve the desirable catalytic activity, especially for improving the OER performances in the acidic solutions. Thus, the innovative design and synthetic approaches are need to be further explored for the development of electrocatalysts

with unique morphologies, which can possess large surface areas to provide more exposed active sites, and thus enhanced electrocatalytic performances [162, 164]. Second, the determinations of active sites and exact location of heteroatoms in nanocarbons are extremely challenging as they can largely effect the electrocatalytic activities [9]. Thus, the development of more advanced characterization techniques, including extended X-ray absorption fine structure, aberration-corrected transmission electron microscopy, and X-ray absorption near edge structure, etc. are required to accurately identify the active sites and location of heteroatoms. Third, the estimation of electrocatalytic activity and feasibility of noble metal-free 2D carbon-based materials in electrolyzers are necessary for practical applications [165]. Therefore, it is required to establish some critical evaluation indicators and standard protocols for the test of activity and durability in practical devices [166]. Last but not least, the reaction mechanisms and kinetics of 2D carbon-based electrocatalysts are still need to be further studied, which play major role in the design of high-performing materials [164]. Therefore, the combined experimental and theoretical approaches are significantly powerful to understand the clear mechanism and basic sciences behind electrocatalysis. In this sense, in situ spectroscopies including in situ Raman, in situ Fourier-transform infrared spectroscopy, and in situ electron spin resonance, with DFT calculations might be valid for further understanding of the reaction mechanisms and kinetics.

Based on the above descriptions, we hope that much more attention should be paid on the development of low cost production methods for the preparation of 2D carbon based materials in large quantities, which are essential for the industrialization. For instance, the fabrication cost of graphene sheets are still very high, which need to be reduced by the advancement of affordable and sophisticated production technologies [163]. Moreover, the development of advanced electrocatalysts with numerous interior defects by creating vacancies of metal or non-metal elements will be an interesting and meaningful research direction for the immediate future [167]. In addition, more studies should be focused on the synthesis of novel 2D flexible nanostructured materials possessing higher mechanical and chemical strengths as well as shape conformability, leading to long term durability under harsh conditions, which is becoming necessary for their utilization in foldable, bendable, portable and even wearable energy related systems [69, 168]. Also, new multiscale hierarchical structures of 2D nanocarbons with high carrier mobility and enhanced physiosorption interaction will play an indispensable and prominent role in their commercialization for water electrolyzers. For example, covalent organic frameworks (COFs)/metal organic frameworks (MOFs) hybrids have not been widely explored, which could possess highly dispersed open active sites, enhanced diffusion of substrates/products, and fast reaction rates, and thus the COFs/MOFs hybrids may be one of the most potential alternatives to replace noble metal-based materials for electrochemical water splitting [169]. Moreover, the continued research in the field of noble metal-free 2D carbon-based materials will give more opportunities for their utilization in other energy related applications including photoelectrochemical water splitting, hydrogen storage, CO_2 reduction, nitrogen reduction, fuel cells, and so on.

Overall, this review offers the recent research progresses of noble-metal-free 2D carbon-based electrocatalysts for HER, OER, and overall water splitting, which could help researchers to master the updated study on the latest 2D nanocarbons and design the high performance electrocatalysts. Also, the synthetic strategies and performances of 2D nanocarbons are highlighted in this review, which could be helpful to revolutionize the future energy systems and should result in healthy environment with less harmful emission of gases, low cost industrial chemical production, better fuel economy, and a less reliance on petroleum products.

Abbreviations

HER: hydrogen evolution reaction; OER: oxygen evolution reaction; 2D: two dimensional; g-C_3N_4: graphitic carbon nitrides; 1D: one dimensional; CNTs: carbon nanotubes; 3D: three dimensional; PCNs: porous carbon nanosheets; H_2: hydrogen; O_2: oxygen; rGO: reduced graphene oxide; GO: graphene oxide; NMPG: N-doped mesoporous graphene; NDGs: pyridinic-N dominated doped graphenes; PANI: polyaniline; NFGNs: N, F co-doped graphene nanosheets; DFT: density functional theory SHG: N, S-doped graphitic sheets; NOGB: N, O co-doped graphene nanorings-integrated boxes; NHPCNs: N-doped hierarchically porous carbon nanosheets; NOMC: N-doped ordered mesoporous carbon; NPs: nanoparticles; NPMC: N, P co-doped mesoporous carbons; Co-NMC: Co, N-doped carbon; DRPC: defect-rich porous carbon; CPT: cathodic polarization treatment; MoS_2: bulk molybdenum disulfide; FeP: iron phosphide; NRGO: N-doped reduced graphene oxide; C_3N_4@NG: a metal-free hybrid composed of g-C_3N_4 and N-doped graphene; SNGS: S, N co-doped porous graphene sheets; CoP@NPMG: a hybrid consisting of the CoP NPs and P, N co-doped mesoporous graphene-like carbon; CoO_x@CN: a cobalt–cobalt oxide with N-doped carbon-based electrocatalyst; LDH: layered double hydroxide; FeOOH: iron oxyhydroxide; FeN_4: iron nitride; VCNs: vertically aligned carbon nanosheets; LDH-NS: layered double hydroxide nanosheets; CVD: chemical vapor deposition; EBP: exfoliated black phosphorous; COFs: covalent organic frameworks; MOFs: metal organic frameworks.

Acknowledgements

Thanks to Head, College of Chemical and Biological Engineering, Zhejiang University, China for kind support for providing necessary facilities.

Authors' contributions

YH and XLF conceived and designed the structure and outline of the manuscript. MAY and LSL wrote the manuscript with the support of QZ and PZ. CJL designed the figures and contributed in drafting the sections related to oxygen evolution reaction. BY, ZJL, and LCL helped in writing the introduction and conclusions sections and provided valuable discussions during the whole drafting process. All authors discussed the manuscript content and contributed to write and revise the paper. All authors read and approved the final manuscript.

Funding
This work was financially supported by National Natural Science Foundation of China (51702284, 21878270, and 21922811), Zhejiang Provincial Natural Science Foundation of China (LR19B060002), and the Startup Foundation for Hundred-Talent Program of Zhejiang University. The funding bodies provided support for the design of the study, analysis and interpretation of data and in writing the manuscript.

Availability of data and materials
Not applicable.

Competing interests
The authors declare that they have no competing interests.

Author details
[1] Key Laboratory of Biomass Chemical Engineering of Ministry of Education, College of Chemical and Biological Engineering, Zhejiang University, Hangzhou 310027, China. [2] Center for Advancing Electronics Dresden (CFAED) and Department of Chemistry and Food Chemistry, Technische Universität Dresden, Mommsenstrasse 4, 01062 Dresden, Germany. [3] Institute of Zhejiang University – Quzhou, 78 Jiuhua Boulevard North, Quzhou 324000, China. [4] School of Petroleum and Chemical Engineering, Dalian University of Technology, Panjin Campus, No. 2 Dagong Road, New District of Liaodong Bay, Panjin City 124221, Liaoning Province, China. [5] Ningbo Research Institute, Zhejiang University, Ningbo 315100, China.

Received: 4 June 2019 Accepted: 25 November 2019
Published online: 17 December 2019

References

1. Yan Y, Xia BY, Zhao B, Wang X. A review on noble-metal-free bifunctional heterogeneous catalysts for overall electrochemical water splitting. J Mater Chem A. 2016;4:17587–603.
2. Marković N, Schmidt T, Stamenković V, Ross P. Oxygen reduction reaction on Pt and Pt bimetallic surfaces: a selective review. Fuel Cells. 2001;1:105–16.
3. Trasatti S. Physical electrochemistry of ceramic oxides. Electrochim Acta. 1991;36:225–41.
4. Antolini E. Palladium in fuel cell catalysis. Energy Environ Sci. 2009;2:915–31.
5. Anantharaj S, Ede SR, Sakthikumar K, Karthick K, Mishra S, Kundu S. recent trends and perspectives in electrochemical water splitting with an emphasis on sulfide, selenide, and phosphide catalysts of Fe Co, and Ni: a review. ACS Catal. 2016;6:8069–97.
6. Lei C, Chen H, Cao J, Yang J, Qiu M, Xia Y, et al. Fe-N_4 sites embedded into carbon nanofiber integrated with electrochemically exfoliated graphene for oxygen evolution in acidic medium. Adv Energy Mater. 2018;8:1801912.
7. Dai L, Xue Y, Qu L, Choi HJ, Baek JB. Metal-free catalysts for oxygen reduction reaction. Chem Rev. 2015;115:4823–92.
8. Yu D, Wei L, Jiang W, Wang H, Sun B, Zhang Q, et al. Nitrogen doped holey graphene as an efficient metal-free multifunctional electrochemical catalyst for hydrazine oxidation and oxygen reduction. Nanoscale. 2013;5:3457–64.
9. Hu C, Xiao Y, Zou Y, Dai L. Carbon-based metal-free electrocatalysis for energy conversion, energy storage, and environmental protection. Electrochem Energy Rev. 2018;1:84–112.
10. Zou X, Zhang Y. Noble metal-free hydrogen evolution catalysts for water splitting. Chem Soc Rev. 2015;44:5148–80.
11. Yan Y, Xia B, Xu Z, Wang X. Recent development of molybdenum sulfides as advanced electrocatalysts for hydrogen evolution reaction. ACS Catal. 2014;4:1693–705.
12. Chen WF, Muckerman JT, Fujita E. Recent developments in transition metal carbides and nitrides as hydrogen evolution electrocatalysts. Chem Commun. 2013;49:8896–909.
13. Xiao P, Chen W, Wang X. A review of phosphide-based materials for electrocatalytic hydrogen evolution. Adv Energy Mater. 2015;5:1500985.
14. Chen X, Gao P, Liu H, Xu J, Zhang B, Zhang Y, et al. In situ growth of iron-nickel nitrides on carbon nanotubes with enhanced stability and activity for oxygen evolution reaction. Electrochim Acta. 2018;267:8–14.
15. Chen Z, Ha Y, Liu Y, Wang H, Yang H, Xu H, et al. In situ formation of cobalt nitrides/graphitic carbon composites as efficient bifunctional electrocatalysts for overall water splitting. ACS Appl Mater Interfaces. 2018;10:7134–44.
16. Zhu Y, Zhou W, Shao Z. Perovskite/carbon composites: applications in oxygen electrocatalysis. Small. 2017;13:1603793.
17. Liu P, Rodriguez JA. Catalysts for hydrogen evolution from the [nife] hydrogenase to the Ni2P(001) surface: the importance of ensemble effect. J Am Chem Soc. 2005;127:14871–8.
18. Chen WF, Sasaki K, Ma C, Frenkel AI, Marinkovic N, Muckerman JT, et al. Hydrogen-evolution catalysts based on non-noble metal nickel–molybdenum nitride nanosheets. Angw Chem Int Ed. 2012;51:6131–5.
19. Vrubel H, Hu X. Molybdenum boride and carbide catalyze hydrogen evolution in both acidic and basic solutions. Angw Chem Int Ed. 2012;51:12703–6.
20. Kong D, Wang H, Cha JJ, Pasta M, Koski KJ, Yao J, et al. Synthesis of MoS_2 and $MoSe_2$ films with vertically aligned layers. Nano Lett. 2013;13:1341–7.
21. Wang J, Cui W, Liu Q, Xing Z, Asiri AM, Sun X. Recent progress in cobalt-based heterogeneous catalysts for electrochemical water splitting. Adv Mater. 2016;28:215–30.
22. Liang Y, Li Y, Wang H, Zhou J, Wang J, Regier T, et al. Co_3O_4 nanocrystals on graphene as a synergistic catalyst for oxygen reduction reaction. Nat Mater. 2011;10:780.
23. McCrory CCL, Jung S, Peters JC, Jaramillo TF. Benchmarking heterogeneous electrocatalysts for the oxygen evolution reaction. J Am Chem Soc. 2013;135:16977–87.
24. Ke J, Adnan Younis M, Kong Y, Zhou H, Liu J, Lei L, et al. Nanostructured ternary metal tungstate-based photocatalysts for environmental purification and solar water splitting: a review. Nano-Micro Lett. 2018;10:69.
25. Keun SK, Zhao Y, Houk J, Sang YL, Jong MK, Kwang SK, et al. Large-scale pattern growth of graphene films for stretchable transparent electrodes. Nature. 2009;457:706.
26. Geim AK, Novoselov KS. The rise of graphene. Nat Mater. 2007;6:183.
27. Zarrin H, Chen Z. Nanocarbons and their hybrids as electrocatalysts for metal-air batteries. Nanocarbons Adv Energy Convers. 2015;2:177–214.
28. Chuangang H, Liming D. Carbon-based metal-free catalysts for electrocatalysis beyond the ORR. Angw Chem Int Ed. 2016;55:11736–58.
29. Wang X, Vasileff A, Jiao Y, Zheng Y, Qiao SZ. Electrnoic and structural engineering of carbon-based metal-free electrocatalysts for water splitting. Adv Mater. 2019;31:1803625.
30. Tian GL, Zhao MQ, Yu D, Kong XY, Huang JQ, Zhang Q, et al. Nitrogen-doped graphene/carbon nanotube hybrids: in situ formation on bifunctional catalysts and their superior electrocatalytic activity for oxygen evolution/reduction reaction. Small. 2014;10:2251–9.
31. He Y, Zhuang X, Lei C, Lei L, Hou Y, Mai Y, et al. Porous carbon nanosheets: synthetic strategies and electrochemical energy related applications. Nano Today. 2019;24:103–19.
32. Ni J, Li Y. Carbon nanomaterials in different dimensions for electrochemical energy storage. Adv Energy Mater. 2016;6:1600278.
33. Paul R, Du F, Dai L, Ding Y, Wang ZL, Wei F, et al. 3D heteroatom-doped carbon nanomaterials as multifunctional metal-free catalysts for integrated energy devices. Adv Mater. 2019;31:1805598.
34. Hou Y, Qiu M, Zhang T, Ma J, Liu S, Zhuang X, et al. Efficient electrochemical and photoelectrochemical water splitting by a 3d nanostructured carbon supported on flexible exfoliated graphene foil. Adv Mater. 2017;29:1604480.
35. Chen M, Guan R, Yang S. Hybrids of fullerenes and 2d nanomaterials. Adv Sci. 2019;6:1800941.
36. Wu G, Santandreu A, Kellogg W, Gupta S, Ogoke O, Zhang H, et al. Carbon nanocomposite catalysts for oxygen reduction and evolution reactions: from nitrogen doping to transition-metal addition. Nano Energy. 2016;29:83–110.
37. Avouris P, Dimitrakopoulos C. Graphene: synthesis and applications. Mater Today. 2012;15:86–97.
38. Balandin AA. Thermal properties of graphene and nanostructured carbon materials. Nat Mater. 2011;10:569.

39. Balandin AA, Ghosh S, Bao W, Calizo I, Teweldebrhan D, Miao F, et al. Superior thermal conductivity of single-layer graphene. Nano Lett. 2008;8:902–7.
40. Kim P, Shi L, Majumdar A, McEuen PL. Thermal transport measurements of individual multiwalled nanotubes. Phys Rev Lett. 2001;87:215502.
41. Alwarappan S, Erdem A, Liu C, Li CZ. Probing the electrochemical properties of graphene nanosheets for biosensing applications. J Phys Chem C. 2009;113:8853–7.
42. Brownson DAC, Kampouris DK, Banks CE. An overview of graphene in energy production and storage applications. J Power Sources. 2011;196:4873–85.
43. Zhou BX, Ding SS, Zhang BJ, Xu L, Chen RS, Luo L, et al. Dimensional transformation and morphological control of graphitic carbon nitride from water-based supramolecular assembly for photocatalytic hydrogen evolution: from 3D to 2D and 1D nanostructures. Appl Catal B Environ. 2019;254:321–8.
44. Duan J, Chen S, Jaroniec M, Qiao SZ. Heteroatom-doped graphene-based materials for energy-relevant electrocatalytic processes. ACS Catal. 2015;5:5207–34.
45. Liang Y, Li Y, Wang H, Dai H. Strongly coupled inorganic/nanocarbon hybrid materials for advanced electrocatalysis. J Am Chem Soc. 2013;135:2013–36.
46. Jiao Y, Zheng Y, Jaroniec M, Qiao SZ. Design of electrocatalysts for oxygen- and hydrogen-involving energy conversion reactions. Chem Soc Rev. 2015;44:2060–86.
47. Li J, Zheng G. One-dimensional earth-abundant nanomaterials for water-splitting electrocatalysts. Adv Sci. 2017;4:1600380.
48. Liu KH, Zhong HX, Li SJ, Duan YX, Shi MM, Zhang XB, et al. Advanced catalysts for sustainable hydrogen generation and storage via hydrogen evolution and carbon dioxide/nitrogen reduction reactions. Prog Mater Sci. 2018;92:64–111.
49. Yang Z, Jing Z, Liangti Q. Graphitic carbon nitride/graphene hybrids as new active materials for energy conversion and storage. ChemNanoMat. 2015;1:298–318.
50. Zhang L, Xiao J, Wang H, Shao M. Carbon-based electrocatalysts for hydrogen and oxygen evolution reactions. ACS Catal. 2017;7:7855–65.
51. Wang T, Zhao Q, Fu Y, Lei C, Yang B, Li Z, et al. Carbon-rich nonprecious metal single atom electrocatalysts for CO_2 reduction and hydrogen evolution. Small Methods;0:1900210.
52. Novoselov KS, Geim AK, Morozov SV, Jiang D, Zhang Y, Dubonos SV, et al. Electric field effect in atomically thin carbon films. Science. 2004;306:666–9.
53. Zhu YP, Guo CX, Zheng Y, Qiao SZ. Surface and interface engineering of noble-metal-free electrocatalysts for efficient energy conversion processes. Acc Chem Res. 2017;50:915–23.
54. Tang C, Wang HF, Chen X, Li BQ, Hou TZ, Zhang B, et al. Topological defects in metal-free nanocarbon for oxygen electrocatalysis. Adv Mater. 2016;28:6845–51.
55. Liu Y, Yu H, Quan X, Chen S, Zhao H, Zhang Y. Efficient and durable hydrogen evolution electrocatalyst based on nonmetallic nitrogen doped hexagonal carbon. Sci Rep. 2014;4:6843.
56. Paul R, Zhu L, Chen H, Qu J, Dai L. Recent advances in carbon-based metal-free electrocatalysts. Adv Mater. 2019;31:1806403.
57. Julkapli NM, Bagheri S. Graphene supported heterogeneous catalysts: an overview. Int J Hydrogen Energy. 2015;40:948–79.
58. Ábrahám D, Nagy B, Dobos G, Madarász J, Onyestyák G, Trenikhin MV, et al. Hydroconversion of acetic acid over carbon aerogel supported molybdenum catalyst. Microporous Mesoporous Mater. 2014;190:46–53.
59. Sakamoto Y, Kaneda M, Terasaki O, Zhao DY, Kim JM, Stucky G, et al. Direct imaging of the pores and cages of three-dimensional mesoporous materials. Nature. 2000;408:449–53.
60. Zheng Y, Liu J, Liang J, Jaroniec M, Qiao SZ. Graphitic carbon nitride materials: controllable synthesis and applications in fuel cells and photocatalysis. Energy Environ Sci. 2012;5:6717–31.
61. Choudhary N, Islam MA, Kim JH, Ko TJ, Schropp A, Hurtado L, et al. Two-dimensional transition metal dichalcogenide hybrid materials for energy applications. Nano Today. 2018;19:16–40.
62. Xiu S, Yao J, Wu G, Huang Y, Yang B, Huang Y, et al. Hydrogen-mediated electron transfer in hybrid microbial-inorganic systems and application in energy and the environment. Energy Technol. 2019;7:1800987.
63. Balun Kayan D, Koçak D, İlhan M. Electrocatalytic hydrogen production on GCE/RGO/Au hybrid electrode. Int J Hydrogen Energy. 2018;43:10562–8.
64. Kumar P, Boukherroub R, Shankar K. Sunlight-driven water-splitting using two-dimensional carbon based semiconductors. J Mater Chem A. 2018;6:12876–931.
65. Song L, Liu Z, Reddy ALM, Narayanan NT, Taha TJ, Peng J, et al. Binary and ternary atomic layers built from carbon, boron, and nitrogen. Adv Mater. 2012;24:4878–95.
66. Sathe BR, Zou X, Asefa T. Metal-free B-doped graphene with efficient electrocatalytic activity for hydrogen evolution reaction. Catal Sci Technol. 2014;4:2023–30.
67. Wasalathilake KC, Ayoko GA, Yan C. Effects of heteroatom doping on the performance of graphene in sodium-ion batteries: a density functional theory investigation. Carbon. 2018;140:276–85.
68. Dou C, Saito S, Matsuo K, Hisaki I, Yamaguchi S. A boron-containing pah as a substructure of boron-doped graphene. Angw Chem Int Ed. 2012;51:12206–10.
69. Jiayuan L, Zeqiong Z, Yuanyuan M, Yongquan Q. Graphene and their hybrid electrocatalysts for water splitting. ChemCatChem. 2017;9:1554–68.
70. Zheng Y, Jiao Y, Ge L, Jaroniec M, Qiao SZ. Two-step boron and nitrogen doping in graphene for enhanced synergistic catalysis. Angw Chem Int Ed. 2013;52:3110–6.
71. Shervedani RK, Amini A. Sulfur-doped graphene as a catalyst support: influences of carbon black and ruthenium nanoparticles on the hydrogen evolution reaction performance. Carbon. 2015;93:762–73.
72. Huang X, Zhao Y, Ao Z, Wang G. Micelle-template synthesis of nitrogen-doped mesoporous graphene as an efficient metal-free electrocatalyst for hydrogen production. Sci Rep. 2014;4:7557.
73. Liang J, Jiao Y, Jaroniec M, Qiao SZ. Sulfur and nitrogen dual-doped mesoporous graphene electrocatalyst for oxygen reduction with synergistically enhanced performance. Angw Chem Int Ed. 2012;51:11496–500.
74. Jiao Y, Zheng Y, Davey K, Qiao SZ. Activity origin and catalyst design principles for electrocatalytic hydrogen evolution on heteroatom-doped graphene. Nat Energy. 2016;1:16130.
75. Zheng Y, Jiao Y, Li LH, Xing T, Chen Y, Jaroniec M, et al. Toward design of synergistically active carbon-based catalysts for electrocatalytic hydrogen evolution. ACS Nano. 2014;8:5290–6.
76. Ito Y, Tanabe Y, Qiu HJ, Sugawara K, Heguri S, Tu NH, et al. High-quality three-dimensional nanoporous graphene. Angw Chem Int Ed. 2014;53:4822–6.
77. Ito Y, Qiu HJ, Fujita T, Tanabe Y, Tanigaki K, Chen M. Bicontinuous nanoporous N-doped graphene for the oxygen reduction reaction. Adv Mater. 2014;26:4145–50.
78. Nørskov JK, Bligaard T, Rossmeisl J, Christensen CH. Towards the computational design of solid catalysts. Nat Chem. 2009;1:37.
79. Greeley J, Jaramillo TF, Bonde J, Chorkendorff I, Nørskov JK. Computational high-throughput screening of electrocatalytic materials for hydrogen evolution. Nat Mater. 2006;5:909.
80. Nørskov JK, Bligaard T, Logadottir A, Kitchin J, Chen JG, Pandelov S, et al. Trends in the exchange current for hydrogen evolution. J Electrochem Soc. 2005;152:J23–6.
81. Yang HB, Miao J, Hung SF, Chen J, Tao HB, Wang X, et al. Identification of catalytic sites for oxygen reduction and oxygen evolution in N-doped graphene materials: development of highly efficient metal-free bifunctional electrocatalyst. Sci Adv. 2016;2:1501122.
82. Wang HF, Tang C, Zhang Q. Template growth of nitrogen-doped mesoporous graphene on metal oxides and its use as a metal-free bifunctional electrocatalyst for oxygen reduction and evolution reactions. Catal Today. 2018;301:25–31.
83. Lin Z, Waller GH, Liu Y, Liu M, Wong C. Simple preparation of nanoporous few-layer nitrogen-doped graphene for use as an efficient electrocatalyst for oxygen reduction and oxygen evolution reactions. Carbon. 2013;53:130–6.
84. Wang Q, Ji Y, Lei Y, Wang Y, Wang Y, Li Y, et al. Pyridinic-N-dominated doped defective graphene as a superior oxygen electrocatalyst for ultrahigh-energy-density Zn-air batteries. ACS Energy Lett. 2018;3:1183–91.

85. Jia Y, Zhang L, Du A, Gao G, Chen J, Yan X, et al. Defect Graphene as a trifunctional catalyst for electrochemical reactions. Adv Mater. 2016;28:9532–8.
86. Lu Z, Wang J, Huang S, Hou Y, Li Y, Zhao Y, et al. N, B-codoped defect-rich graphitic carbon nanocages as high performance multifunctional electrocatalysts. Nano Energy. 2017;42:334–40.
87. Li R, Wei Z, Gou X. Nitrogen and phosphorus dual-doped graphene/carbon nanosheets as bifunctional electrocatalysts for oxygen reduction and evolution. ACS Catal. 2015;5:4133–42.
88. Li X, Duan X, Han C, Fan X, Li Y, Zhang F, et al. Chemical activation of nitrogen and sulfur co-doped graphene as defect-rich carbocatalyst for electrochemical water splitting. Carbon. 2019;148:540–9.
89. Zhang J, Dai L. Nitrogen, phosphorus, and fluorine tri-doped graphene as a multifunctional catalyst for self-powered electrochemical water splitting. Angw Chem Int Ed. 2016;55:13296–300.
90. Yue X, Huang S, Cai J, Jin Y, Shen PK. Heteroatoms dual doped porous graphene nanosheets as efficient bifunctional metal-free electrocatalysts for overall water-splitting. J Mater Chem A. 2017;5:7784–90.
91. Hu C, Dai L. Multifunctional carbon-based metal-free electrocatalysts for simultaneous oxygen reduction, oxygen evolution, and hydrogen evolution. Adv Mater. 2017;29:1604942.
92. Hu Q, Li G, Li G, Liu X, Zhu B, Chai X, et al. Trifunctional electrocatalysis on dual-doped graphene nanorings–integrated boxes for efficient water splitting and Zn-air batteries. Adv Energy Mater. 2019;9:1803867.
93. Lee J, Kim J, Hyeon T. Recent progress in the synthesis of porous carbon materials. Adv Mater. 2006;18:2073–94.
94. Fan H, Shen W. Carbon nanosheets: synthesis and application. Chemsuschem. 2015;8:2004–27.
95. Wang F, Duan W, Wang K, Dong X, Gao M, Zhai Z, et al. Graphitized hierarchically porous carbon nanosheets derived from bakelite induced by high-repetition picosecond laser. Appl Surf Sci. 2018;450:155–63.
96. Jayaramulu K, Dubal DP, Nagar B, Ranc V, Tomanec O, Petr M, et al. Ultrathin hierarchical porous carbon nanosheets for high-performance supercapacitors and redox electrolyte energy storage. Adv Mater. 2018;30:1705789.
97. Lu C, Tranca D, Zhang J, Rodríguez Hernández F, Su Y, Zhuang X, et al. Molybdenum carbide-embedded nitrogen-doped porous carbon nanosheets as electrocatalysts for water splitting in alkaline media. ACS Nano. 2017;11:3933–42.
98. Kim NR, Yun YS, Song MY, Hong SJ, Kang M, Leal C, et al. Citrus-peel-derived, nanoporous carbon nanosheets containing redox-active heteroatoms for sodium-ion storage. ACS Appl Mater Interfaces. 2016;8:3175–81.
99. Dai L. Carbon-based catalysts for metal-free electrocatalysis. Curr Opin Electrochem. 2017;4:18–25.
100. Xia Y, Yang Z, Zhu Y. Porous carbon-based materials for hydrogen storage: advancement and challenges. J Mater Chem A. 2013;1:9365–81.
101. Long GF, Wan K, Liu MY, Liang ZX, Piao JH, Tsiakaras P. Active sites and mechanism on nitrogen-doped carbon catalyst for hydrogen evolution reaction. J Catal. 2017;348:151–9.
102. Yang S, Zhi L, Tang K, Feng X, Maier J, Müllen K. Efficient synthesis of heteroatom (N or S)-doped graphene based on ultrathin graphene oxide-porous silica sheets for oxygen reduction reactions. Adv Funct Mater. 2012;22:3634–40.
103. Yoshikazu I, Weitao C, Takeshi F, Zheng T, Mingwei C. High catalytic activity of nitrogen and sulfur co-doped nanoporous graphene in the hydrogen evolution reaction. Angew Chem Int Ed. 2015;127:2159–64.
104. Li Y, Zhang H, Wang Y, Liu P, Yang H, Yao X, et al. A self-sponsored doping approach for controllable synthesis of S and N co-doped trimodal-porous structured graphitic carbon electrocatalysts. Energy Environ Sci. 2014;7:3720–6.
105. Wei L, Karahan HE, Goh K, Jiang W, Yu D, Birer Ö, et al. A high-performance metal-free hydrogen-evolution reaction electrocatalyst from bacterium derived carbon. J Mater Chem A. 2015;3:7210–4.
106. Zhou Y, Leng Y, Zhou W, Huang J, Zhao M, Zhan J, et al. Sulfur and nitrogen self-doped carbon nanosheets derived from peanut root nodules as high-efficiency non-metal electrocatalyst for hydrogen evolution reaction. Nano Energy. 2015;16:357–66.
107. Liu X, Zhou W, Yang L, Li L, Zhang Z, Ke Y, et al. Nitrogen and sulfur co-doped porous carbon derived from human hair as highly efficient metal-free electrocatalysts for hydrogen evolution reactions. J Mater Chem A. 2015;3:8840–6.
108. Lei C, Wang Y, Hou Y, Liu P, Yang J, Zhang T, et al. Efficient alkaline hydrogen evolution on atomically dispersed Ni–Nx Species anchored porous carbon with embedded Ni nanoparticles by accelerating water dissociation kinetics. Energy Environ Sci. 2018;12:149–56.
109. Zhao Y, Nakamura R, Kamiya K, Nakanishi S, Hashimoto K. Nitrogen-doped carbon nanomaterials as non-metal electrocatalysts for water oxidation. Nat Commun. 2013;4:2390.
110. Pi YT, Xing XY, Lu LM, He ZB, Ren TZ. Hierarchical porous activated carbon in OER with high efficiency. RSC Adv. 2016;6:102422–7.
111. Peng X, Zhang L, Chen Z, Zhong L, Zhao D, Chi X, et al. Hierarchically porous carbon plates derived from wood as bifunctional ORR/OER electrodes. Adv Mater. 2019;31:1900341.
112. Jiang H, Gu J, Zheng X, Liu M, Qiu X, Wang L, et al. Defect-rich and ultrathin N doped carbon nanosheets as advanced trifunctional metal-free electrocatalysts for the ORR, OER and HER. Energy Environ Sci. 2019;12:322–33.
113. Zhang J, Zhao Z, Xia Z, Dai L. A metal-free bifunctional electrocatalyst for oxygen reduction and oxygen evolution reactions. Nat Nanotechnol. 2015;10:444.
114. Fei H, Dong J, Arellano MJ, Ye G, Kim ND, Samuel EL, et al. Atomic cobalt on nitrogen-doped graphene for hydrogen generation. Nat Commun. 2015;6:8668.
115. Bayatsarmadi B, Zheng Y, Tang Y, Jaroniec M, Qiao SZ. Significant enhancement of water splitting activity of n-carbon electrocatalyst by trace level Co doping. Small. 2016;12:3703–11.
116. Hou Y, Qiu M, Kim MG, Liu P, Nam G, Zhang T, et al. Atomically dispersed nickel-nitrogen-sulfur species anchored on porous carbon nanosheets for efficient water oxidation. Nat Commun. 2019;10:1392.
117. Zhang Z, Yi Z, Wang J, Tian X, Xu P, Shi G, et al. Nitrogen-enriched polydopamine analogue-derived defect-rich porous carbon as a bifunctional metal-free electrocatalyst for highly efficient overall water splitting. J Mater Chem A. 2017;5:17064–72.
118. Lei Y, Wei L, Zhai S, Wang Y, Karahan HE, Chen X, et al. Metal-free bifunctional carbon electrocatalysts derived from zeolitic imidazolate frameworks for efficient water splitting. Mater Chem Front. 2018;2:102–11.
119. Jieun Y, Damien V, Joon AS, Dongwoo K, Young KA, Manish C, et al. Two-dimensional hybrid nanosheets of tungsten disulfide and reduced graphene oxide as catalysts for enhanced hydrogen evolution. Angw Chem Int Ed. 2013;52:13751–4.
120. Ma TY, Dai S, Jaroniec M, Qiao SZ. Graphitic carbon nitride nanosheet-carbon nanotube three-dimensional porous composites as high-performance oxygen evolution electrocatalysts. Angw Chem Int Ed. 2014;53:7281–5.
121. Chen S, Qiao SZ. Hierarchically porous nitrogen-doped graphene-$NiCo_2O_4$ hybrid paper as an advanced electrocatalytic water-splitting material. ACS Nano. 2013;7:10190–6.
122. Liu T, Li M, Su Z, Bo X, Guan W, Zhou M. Monodisperse and tiny $Co_2N_{0.67}$ nanocrystals uniformly embedded over two curving surfaces of hollow carbon microfibers as efficient electrocatalyst for oxygen evolution reaction. ACS Appl Nano Mater. 2018;1:4461–73.
123. Kashyap V, Kurungot S. Zirconium-substituted cobalt ferrite nanoparticle supported n-doped reduced graphene oxide as an efficient bifunctional electrocatalyst for rechargeable Zn-air battery. ACS Catal. 2018;8:3715–26.
124. Zhu YP, Guo C, Zheng Y, Qiao SZ. Surface and interface engineering of noble-metal-free electrocatalysts for efficient energy conversion processes. Acc Chem Res. 2017;50:915–23.
125. Liu D, Lu Q, Luo Y, Sun X, Asiri AM. $NiCo_2S_4$ nanowires array as an efficient bifunctional electrocatalyst for full water splitting with superior activity. Nanoscale. 2015;7:15122–6.
126. Xu X, Chu H, Zhang Z, Dong P, Baines R, Ajayan PM, et al. Integrated energy aerogel of N, S-rGO/WSe2/NiFe-LDH for both energy conversion and storage. ACS Appl Mater Interfaces. 2017;9:32756–66.
127. Chen S, Duan J, Ran J, Jaroniec M, Qiao SZ. N-doped graphene film-confined nickel nanoparticles as a highly efficient three-dimensional oxygen evolution electrocatalyst. Energy Environ Sci. 2013;6:3693–9.
128. Li Y, Wang H, Xie L, Liang Y, Hong G, Dai H. MoS_2 nanoparticles grown on graphene: an advanced catalyst for the hydrogen evolution reaction. J Am Chem Soc. 2011;133:7296–9.

129. Zhang Z, Lu B, Hao J, Yang W, Tang J. FeP nanoparticles grown on graphene sheets as highly active non-precious-metal electrocatalysts for hydrogen evolution reaction. Chem Commun. 2014;50:11554–7.
130. Pan Y, Yang N, Chen Y, Lin Y, Li Y, Liu Y, et al. Nickel phosphide nanoparticles-nitrogen-doped graphene hybrid as an efficient catalyst for enhanced hydrogen evolution activity. J Power Sources. 2015;297:45–52.
131. Shinde SS, Sami A, Lee JH. Electrocatalytic hydrogen evolution using graphitic carbon nitride coupled with nanoporous graphene co-doped by S and Se. J Mater Chem A. 2015;3:12810–9.
132. Zheng Y, Jiao Y, Zhu Y, Li LH, Han Y, Chen Y, et al. Hydrogen evolution by a metal-free electrocatalyst. Nat Commun. 2014;5:3783.
133. Shinde SS, Sami A, Lee JH. Nitrogen and phosphorus-doped nanoporous graphene/graphitic carbon nitride hybrids as efficient electrocatalysts for hydrogen evolution. ChemCatChem. 2015;7:3873–80.
134. Cao J, Lei C, Yang B, Li Z, Lei L, Hou Y, et al. Zeolitic imidazolate framework-derived core-shell-structured CoS_2/CoS_2-N-C supported on electrochemically exfoliated graphene foil for efficient oxygen evolution. Batteries Supercaps. 2018;2:348–54.
135. Cao J, Lei C, Yang J, Cheng X, Li Z, Yang B, et al. An ultrathin cobalt-based zeolitic imidazolate framework nanosheet array with a strong synergistic effect towards the efficient oxygen evolution reaction. J Mater Chem A. 2018;6:18877–83.
136. Hou Y, Li J, Wen Z, Cui S, Yuan C, Chen J. Co_3O_4 nanoparticles embedded in nitrogen-doped porous carbon dodecahedrons with enhanced electrochemical properties for lithium storage and water splitting. Nano Energy. 2015;12:1–8.
137. Cheng X, Pan Z, Lei C, Jin Y, Yang B, Li Z, et al. A strongly coupled 3D ternary Fe_2O_3@Ni_2P/$Ni(PO_3)_2$ hybrid for enhanced electrocatalytic oxygen evolution at ultra-high current densities. J Mater Chem A. 2019;7:965–71.
138. Wang J, Yang W, Liu J. CoP_2 nanoparticles on reduced graphene oxide sheets as a super-efficient bifunctional electrocatalyst for full water splitting. J Mater Chem A. 2016;4:4686–90.
139. Zhang X, Liu S, Zang Y, Liu R, Liu G, Wang G, et al. Co/Co9S8@S, N-doped porous graphene sheets derived from S, N dual organic ligands assembled Co-MOFs as superior electrocatalysts for full water splitting in alkaline media. Nano Energy. 2016;30:93–102.
140. Sun Y, Li C, Xu Y, Bai H, Yao Z, Shi G. Chemically converted graphene as substrate for immobilizing and enhancing the activity of a polymeric catalyst. Chem Commun. 2010;46:4740–2.
141. Liu X, Dai L. Carbon-based metal-free catalysts. Nat Rev Mater. 2016;1:16064.
142. Jingqi T, Qian L, Asiri AM, Alamry KA, Xuping S. Ultrathin graphitic C_3N_4 nanosheets/graphene composites: efficient organic electrocatalyst for oxygen evolution reaction. ChemSusChem. 2014;7:2125–30.
143. Cobo S, Heidkamp J, Jacques PA, Fize J, Fourmond V, Guetaz L, et al. A janus cobalt-based catalytic material for electro-splitting of water. Nat Mater. 2012;11:802.
144. Wang P, Song F, Amal R, Ng YH, Hu X. Efficient water splitting catalyzed by cobalt phosphide-based nanoneedle arrays supported on carbon cloth. Chemsuschem. 2016;9:472–7.
145. Jiao L, Zhou Y-X, Jiang HL. Metal-organic framework-based CoP/reduced graphene oxide: high-performance bifunctional electrocatalyst for overall water splitting. Chem Sci. 2016;7:1690–5.
146. Wang X, Li W, Xiong D, Petrovykh DY, Liu L. Bifunctional nickel phosphide nanocatalysts supported on carbon fiber paper for highly efficient and stable overall water splitting. Adv Funct Mater. 2016;26:4067–77.
147. You B, Jiang N, Sheng M, Gul S, Yano J, Sun Y. High-performance overall water splitting electrocatalysts derived from cobalt-based metal–organic frameworks. Chem Mater. 2015;27:7636–42.
148. Hou Y, Qiu M, Zhang T, Zhuang X, Kim CS, Yuan C, et al. Ternary porous cobalt phosphoselenide nanosheets: an efficient electrocatalyst for electrocatalytic and photoelectrochemical water splitting. Adv Mater. 2017;29:1701589.
149. Liu Y, Zhu Y, Shen J, Huang J, Yang X, Li C. CoP nanoparticles anchored on N, P-dual-doped graphene-like carbon as a catalyst for water splitting in non-acidic media. Nanoscale. 2018;10:2603–12.
150. Lin CH, Chen CL, Wang JH. Mechanistic studies of water-gas-shift reaction on transition metals. J Phys Chem C. 2011;115:18582–8.
151. Jin H, Wang J, Su D, Wei Z, Pang Z, Wang Y. In situ cobalt–cobalt oxide/n-doped carbon hybrids as superior bifunctional electrocatalysts for hydrogen and oxygen evolution. J Am Chem Soc. 2015;137:2688–94.
152. Gong M, Zhou W, Tsai MC, Zhou J, Guan M, Lin MC, et al. Nanoscale nickel oxide/nickel heterostructures for active hydrogen evolution electrocatalysis. Nat Commun. 2014;5:4695.
153. Zhang Y, Rui K, Ma Z, Sun W, Wang Q, Wu P, et al. Cost-effective vertical carbon nanosheets/iron-based composites as efficient electrocatalysts for water splitting reaction. Chem Mater. 2018;30:4762–9.
154. Luo J, Im JH, Mayer MT, Schreier M, Nazeeruddin MK, Park NG, et al. Water photolysis at 12.3% efficiency via perovskite photovoltaics and earth-abundant catalysts. Science. 2014;345:1593.
155. Zhao Z, Schipper DE, Leitner AP, Thirumalai H, Chen JH, Xie L, et al. Bifunctional metal phosphide FeMnP films from single source metal organic chemical vapor deposition for efficient overall water splitting. Nano Energy. 2017;39:444–53.
156. Jia Y, Zhang L, Gao G, Chen H, Wang B, Zhou J, et al. A heterostructure coupling of exfoliated Ni–Fe hydroxide nanosheet and defective graphene as a bifunctional electrocatalyst for overall water splitting. Adv Mater. 2017;29:1700017.
157. Ren X, Zhou J, Qi X, Liu Y, Huang Z, Li Z, et al. Few-layer black phosphorus nanosheets as electrocatalysts for highly efficient oxygen evolution reaction. Adv Energy Mater. 2017;7:1700396.
158. Liu H, Neal AT, Zhu Z, Luo Z, Xu X, Tománek D, et al. Phosphorene: an unexplored 2d semiconductor with a high hole mobility. ACS Nano. 2014;8:4033–41.
159. Jiang Q, Xu L, Chen N, Zhang H, Dai L, Wang S. Facile synthesis of black phosphorus: an efficient electrocatalyst for the oxygen evolving reaction. Angew Chem Int Ed. 2016;55:13849–53.
160. Yuan Z, Li J, Yang M, Fang Z, Jian J, Yu D, et al. Ultrathin black phosphorus-on-nitrogen doped graphene for efficient overall water splitting: dual modulation roles of directional interfacial charge transfer. J Am Chem Soc. 2019;141:4972–9.
161. He Y, Gehrig D, Zhang F, Lu C, Zhang C, Cai M, et al. Highly efficient electrocatalysts for oxygen reduction reaction based on 1D ternary doped porous carbons derived from carbon nanotube directed conjugated microporous polymers. Adv Funct Mater. 2016;26:8255–65.
162. Han L, Dong S, Wang E. Transition-metal (Co, Ni, and Fe)-based electrocatalysts for the water oxidation reaction. Adv Mater. 2016;28:9266–91.
163. Deng D, Novoselov KS, Fu Q, Zheng N, Tian Z, Bao X. Catalysis with two-dimensional materials and their heterostructures. Nat Nanotechnol. 2016;11:218.
164. Lyu F, Wang Q, Choi SM, Yin Y. Noble-metal-free electrocatalysts for oxygen evolution. Small. 2019;15:1804201.
165. Lulu Z, Jin X, Haiyan W, Shao M. Carbon-based electrocatalysts for hydrogen and oxygen evolution reactions. ACS Catal. 2017;7:7855–65.
166. Tang C, Titirici MM, Zhang Q. A review of nanocarbons in energy electrocatalysis: multifunctional substrates and highly active sites. J Energy Chem. 2017;26:1077–93.
167. Yan D, Li Y, Huo J, Chen R, Dai L, Wang S. Defect chemistry of nonprecious-metal electrocatalysts for oxygen reactions. Adv Mater. 2017;29:1606459.
168. Ma TY, Ran J, Dai S, Jaroniec M, Qiao SZ. Phosphorus-doped graphitic carbon nitrides grown in situ on carbon-fiber paper: flexible and reversible oxygen electrodes. Angw Chem Int Ed. 2015;54:4646–50.
169. Yan Y, He T, Zhao B, Qi K, Liu H, Xia BY. Metal/covalent-organic frameworks-based electrocatalysts for water splitting. J Mater Chem A. 2018;6:15905–26.
170. Hou Y, Huang T, Wen Z, Mao S, Cui S, Chen J. Metal-organic framework-derived nitrogen-doped core-shell-structured porous Fe/Fe_3C@C nanoboxes supported on graphene sheets for efficient oxygen reduction reactions. Adv Energy Mater. 2014;4:1400337.
171. Zhang J, Qu L, Shi G, Liu J, Chen J, Dai L. N, P-codoped carbon networks as efficient metal-free bifunctional catalysts for oxygen reduction and hydrogen evolution reactions. Angw Chem Int Ed. 2016;55:2230–4.
172. Ito Y, Cong W, Fujita T, Tang Z, Chen M. High catalytic activity of nitrogen and sulfur co-doped nanoporous graphene in the hydrogen evolution reaction. Angw Chem Int Ed. 2015;54:2131–6.
173. Jiao D, Pengju R, Dehui D, Xinhe B. Enhanced electron penetration through an ultrathin graphene layer for highly efficient catalysis of the hydrogen evolution reaction. Angew Chem Int Ed. 2015;54:2100–4.

174. Li M, Liu X, Xiong Y, Bo X, Zhang Y, Han C, et al. Facile synthesis of various highly dispersive CoP nanocrystal embedded carbon matrices as efficient electrocatalysts for the hydrogen evolution reaction. J Mater Chem A. 2015;3:4255–65.
175. Yang L, Yu J, Wei Z, Li G, Cao L, Zhou W, et al. Co-N-doped MoO_2 nanowires as efficient electrocatalysts for the oxygen reduction reaction and hydrogen evolution reaction. Nano Energy. 2017;41:772–9.
176. Xu Y, Tu W, Zhang B, Yin S, Huang Y, Kraft M, et al. Nickel nanoparticles encapsulated in few-layer nitrogen-doped graphene derived from metal–organic frameworks as efficient bifunctional electrocatalysts for overall water splitting. Adv Mater. 2017;29:1605957.
177. Fan X, Peng Z, Ye R, Zhou H, Guo X. M3C (M: Fe Co, Ni) nanocrystals encased in graphene nanoribbons: an active and stable bifunctional electrocatalyst for oxygen reduction and hydrogen evolution reactions. ACS Nano. 2015;9:7407–18.
178. Yipu L, Guangtao Y, Guo-Dong L, Yuanhui S, Tewodros A, Wei C, et al. Coupling Mo_2C with nitrogen-rich nanocarbon leads to efficient hydrogen-evolution electrocatalytic sites. Angw Chem Int Ed. 2015;54:10752–7.
179. Zhao M, Zhang J, Xiao H, Hu T, Jia J, Wu H. Facile in situ synthesis of a carbon quantum dot/graphene heterostructure as an efficient metal-free electrocatalyst for overall water splitting. Chem Commun. 2019;55:1635–8.
180. Liu M-R, Hong QL, Li QH, Du Y, Zhang HX, Chen S, et al. Cobalt boron imidazolate framework derived cobalt nanoparticles encapsulated in B/N codoped nanocarbon as efficient bifunctional electrocatalysts for overall water splitting. Adv Funct Mater. 2018;28:1801136.
181. Tahir M, Mahmood N, Zhang X, Mahmood T, Butt FK, Aslam I, et al. Bifunctional catalysts of Co_3O_4@GCN tubular nanostructured (TNS) hybrids for oxygen and hydrogen evolution reactions. Nano Res. 2015;8:3725–36.
182. Ma TY, Dai S, Jaroniec M, Qiao SZ. Metal-organic framework derived hybrid Co_3O_4-carbon porous nanowire arrays as reversible oxygen evolution electrodes. J Am Chem Soc. 2014;136:13925–31.
183. Zhang X, Xu H, Li X, Li Y, Yang T, Liang Y. Facile synthesis of nickel-iron/nanocarbon hybrids as advanced electrocatalysts for efficient water splitting. ACS Catal. 2016;6:580–8.
184. Zhang S, Yu X, Yan F, Li C, Zhang X, Chen Y. N-Doped graphene-supported Co@CoO core-shell nanoparticles as high-performance bifunctional electrocatalysts for overall water splitting. J Mater Chem A. 2016;4:12046–53.

Publisher's Note